School of Physics & Astronomy Queen Mary University of London

An analysis of the Keeler Gap

Sophie-Lynne Jory (130349644)

Supervised by Prof C.D. Murray

Submitted August 2018 in part fulfilment of the requirements for the degree of Master in Astrophysics at Queen Mary University of London

Declaration

I hereby certify that this Dissertation, which is approximately 10000 thousand words in length, has been written by me at the School of Physics and Astronomy, Queen Mary University of London, that all material in this dissertation which is not my own work has been properly acknowledged, and that it has not been submitted in any previous application for a higher degree.

The sections which contain the report on the independent research work component of the project are Chapter 2-4

Sophie-Lynne Jory (130349644)

Acknowledgements

I would like to wish a special thanks my supevisor, Prof. C. D. Murray, for his guidance, constructive criticism and granting me the opportunity to work on a project that his lectures inspired me pursue. I would like to thank Dr R. A. Jacobson for permission to see and use information from his internal memo at JPL/Caltech. I would like to express my appreciation for the encouragement and technical support provided by Dr. N. Cooper.

Abstract

The Keeler Gap is a 37km gap near the outer edge of Saturn's A ring. It has a collection of unusual features including a moon, Daphnis. This moon causes further features to arise, such as edge waves. Previous research suggests that Daphnis is not alone in the Keeler Gap. The waves of the Keeler Gap don't decay as the analytical expression predicts [5] and the orbit of Daphnis has changed at least twice since it was first observed[3]. We analysed a strategically chosen selection of Image from the Cassini spacecraft with the aim of gaining deeper understanding of what leads to the changes in Daphnis' orbit while making note and exploring any new features observed. We calculated that an object (in a horseshoe orbit) within the Keeler Gap causing this orbital disruption, would have to have a radius $> 570\pm360$ m which corresponds to a mass $> 2.7 \pm 0.5 \times 10^{11}$ kg. We observed numerous anomalously bright pixels in the Keeler Gap (in individual images as well as a mosaic). We calculated mean motions for these anomalies and found that some had a mean motion corresponding to what you would expect for an object in the Keeler $Gap(\sim 605 \text{ deg/day})$. We measured the decay of the Keeler Gap edge waves and found sudden increases in amplitudes of the waves in some cases and in one case, we found outer edge waves where none were predicted. All methods used in this report suggest that Daphnis may not alone in the Keeler Gap, this echoes the findings of previous research. The mean motion calculations and the mosaic suggest that there may be more than one object present.

Contents

Li	st of	Figures	viii
Li	st of	Tables	x
1.	Intr	oduction	1
	1.1.	Background	1
		1.1.1. Cassini	1
		Image Flaws	2
		1.1.2. Encke Gap	2
		Edge Waves	3
		Pan	3
		1.1.3. Keeler Gap	4
		1.1.4. Daphnis	4
		Discovery	4
		Effect on Keeler Gap	5
		Properties	5
		Behaviour	5
		1.1.5. Software	5
2.	Met	chod	9
	2.1.	Strategies, selection	9
		2.1.1. Criteria	9
		2.1.2. Daphnis targeted images	9
		2.1.3. Indirect observation	10
	2.2.	Brute Force Searching	10
	2.3.	Possible avenues	10
	2.4.	Orbit Predictions	11
		2.4.1. The Calculation	11
	2.5.	Calculated Constraints	13
	2.6	Points of Interest	14

3.	Res	${ m ults}$		16
	3.1.	Bright	Dots and their Mean Motions	16
		3.1.1.	Candidate Images	16
			Image C \dots	16
			Image D	16
			Image E	16
			${\rm Image}\ F\ \dots$	19
			Image G \dots	19
			Image H	20
			Image I	22
			Image J	22
		3.1.2.	Possible background star	23
	3.2.	Propel	ller	23
	3.3.	Waves	at the Keeler Gap edge	25
		3.3.1.	N1612090521: DN vs True Longitude graph $\dots \dots \dots$	26
		3.3.2.	N1630270620: DN vs True Longitude graph	27
		3.3.3.	Motion of peak between subsequent images	29
		3.3.4.	N1630270653: DN vs True Longitude graph	30
	3.4.	Mosaid	cs	31
			N158497* Mosaic	31
	3.5.	Discus	sion	32
		3.5.1.	Mass and Radius Constraints	32
		3.5.2.	DN vs True Longitude Graphs	33
		3.5.3.	Mosaic	34
		3.5.4.	Other images	34
		3.5.5.	Mean Motion	35
			E-F	35
			I-J	35
			G-H	35
			H-I	35
			G-I	36
			C-D	36
4	Con	clusio	n	37
	C011		Future Research	
Ri	hling	ranhv		40

Appendices	42
A. Other Images	43

List of Figures

1.1.	Daphnis close up, Image Name = N1863267232; Target = Daphnis;	
	Image Mid-Time = $2017-016$ $13:06:18.761$ UTC; Exposure = $460s$;	
	$Radial\ Resolution = 0.3461.\ Image\ Credit:\ NASA/JPL-Caltech/Space$	
	Science Institute	6
1.2.	Screenshot of the Caviar Software Window with a pointed image. The	
	Cassini image in the example is N1612038605. Later in this report	
	it is labelled as Image G. For image details, see Table 3.1. Image	
	Credit: NASA/JPL-Caltech/Space Science Institute	7
2.1.	This diagram shows a close up of the change in orbital radius, Δa , of	
	two masses, m_1 and m_2 , as they approach each other in their orbits.	
	This is from a co-orating perspective. The initial and final locations	
	are indicated by the subscript "i" and "f" respectively. The dotted	
	line indicates a midpoint in the orbit	13
3.1.	Image C (Cropped and magnified); For image details, see Table 3.1.	
	Image Credit: NASA/JPL-Caltech/Space Science Institute	16
3.2.	Image D (cropped); For image details, see Table 3.1. Image Credit:	
	NASA/JPL-Caltech/Space Science Institute	19
3.3.	For image details, see Table 3.1	19
3.4.	Image F (cropped); For image details, see Table 3.1. Image Credit:	
	NASA/JPL-Caltech/Space Science Institute	20
3.5.	For image details, see Table 3.1	20
3.6.	For image details, see Table 3.1	21
3.7.	Image I (cropped); For image details, see Table 3.1. Image Credit:	
	NASA/JPL-Caltech/Space Science Institute	22
3.8.	Image J (cropped); For image details, see Table 3.1. Image Credit:	
	NASA/JPL-Caltech/Space Science Institute	22
3.9.	Image $\alpha,$ Image Credit: NASA/JPL-Caltech/Space Science Institute .	25
3.10	Image \(\text{Image Credit: NASA/IPL-Caltech/Space Science Institute} \)	25

3.11.	N1591068064 Image Credit: NASA/JPL-Caltech/Space Science In-	
	stitute	26
3.12.	Image N1630270620: Inner edge DN values	29
3.13.	Image N1630270620: Outer edge DN values	29
3.14.	Image N1630270620: Both inner and outer edge DN values	29
3.15.	A scatter plot of digital no. vs true longitude (deg) for image N1630270653	3.
	Both inner and outer edge DN values with moving averages	30
3.16.	Mosaic of Images N15849733717-N1584976298	31
3.17.	Mosaic of Images N15849733717-N1584976298 (cropped)	32
3.18.	As a comparison, this is what a group of three stars looks like from	
	another image (before reprojection) in the same sequence, Image	
	N1584974696 Image Credit: NASA/JPL-Caltech/Space Science In-	
	stitute	32
3.19.	Image N1584978784 (cropped)	33
A.1.	For image details, see Table 3.1	43
A.2.	Image L. In this image the variation is barely visible due to the low	
	resolution of the image. For image details, see Table 3.1. Image	
	, 1	44
A.3.	This image had to be stretched (as seen in Fig. A.3b) significantly	
	in order to see the single anomalous pixel. This is very unusual.	
	However the DN value measured for this pixel is second highest of	
	the candidate images. The DN value of the pixel is 218. For image	
		45
A.4.	Image A (cropped), For image details, see Table 3.1. Contribution	
	from Dr N. J. Cooper (personal communication). Image Credit:	
	7 1	46
A.5.	Image B (cropped), For image details, see Table 3.1. Image Credit:	
	NASA/JPL-Caltech/Space Science Institute	46
A.6.	Reprojection of Image N1591067614 (cropped). This bright line is	
	approximately circular in appearance in the raw image but the repro-	
	jection process of the image has distorted it	47

List of Tables

1.1.	Daphnis Planetocentric Equatorial Elements Credit: Jacobson JPL/Caltech[3]	6
2.1.	Testing Excel calculations on targeted images of Daphnis. These calculations are used to predict the location of an object after time	
	interval Δt	
2.2.	Mass and Radius values for Daphnis according to Thomas[4] and	
	Porco[9]	
3.1.	Points of interest and their locations in each image	
3.2.	Mean Motion as calculated between 2 images	
3.3.	Details for images containing the bright object (possible background	
	star)	
3.4.	Locations of bright object (possible background star)	
3.5.	Mean motions of the object between images	

1. Introduction

This project started with an image of Daphnis and a question; "What do you see?" The image shown was the full colour version of what we see in Fig. 1.1a. Daphnis is a moon in the Keeler Gap of Saturn's rings. It was discovered in 2004 but is not fully understood, particularly with regards to its orbital motion and effects on the Keeler Gap. The most striking effect of Daphnis on the Keeler Gap is in the form of edge waves. The waves don't behave as predicted decaying sooner than expected and there are other oscillations that are not caused by Daphnis. Some of this can be explained by resonance from Prometheus[10]. Jacobson made calculations for the orbital elements but found that three fits had to be made to account for the variation in Daphnis' motion[3]. The reason for this variation is not known. This report intends to address these questions by taking measurements from Cassini images using the Caviar software[7] to analyse the decay of Keeler Gap edge waves and making note of any unusual features while strategically searching through the vast collection of images.

1.1. Background

1.1.1. Cassini

The Cassini spacecraft was launched on October 15th 1997[12]. The main mission of the Cassini Spacecraft was to perform many flybys inorder collect data on Saturn, its Moons and its disc. The type of data can be categorised as "Optical Remote Sensing", "Fields, Particles and Waves" and "Microwave Remote sensing"[12]. It wasn't until 2002 that it was able take its first photograph of Saturn 2.85×10^8 km away[12]. This was not the first time that a probe had been sent to take images of Saturn. The first was Pioneer 11 in 1979. Voyager 1 had previously taken 17,078 photographs of Saturn and Voyager 2 had taken 11,972[16].

Cassini has two cameras as part of its Imaging Science Subsystem (ISS). One wide angle and one narrow angle [12]. This was also the case with the Voyager probes but Cassini's on-board imaging system had more filters (18 instead of 8 for the Wide

Angle Camera(WAC) and 24 instead of 8 for the Narrow Angle Camera(NAC)). Cassini also had a 2m focal length NAC whereas the one on Voyager spacecraft 1.5m. [1][12][13] For the purposes of discerning greater detail, Cassini's higher resolution NAC is of great help; the key difference is that Cassini was much closer and took more images of Saturnian objects as well as direct images of Saturn and its rings. Most of the satellorb type images (images taken as part of an effort to photograph small inner satellites of Saturn) were 680ms long exposure although later in the mission, a decision was made to take pairs of photos (680ms exposure and a 150ms exposure). This means that for brighter objects you get 2 images with a very slight difference. This makes it easier to differentiate what is a cosmic ray and what is an actual feature since the anomalous pixel will not appear in both images.

All these factors mean that there was a wealth of new, clearer data that could be used to re-analyse Saturn, its rings and its moons.

Image Flaws Many different types of errors can arise when an image is taken. They can come from external particles, camera imperfections and errors in data transmission. External particles can be something as simple as an incident charged particle such as a cosmic ray. These can appear as anything from a bright pixel to a squiggle shape. Cosmic rays do not appear on their own. It is preferable to describe errors in terms of density of cosmic rays. Longer exposures give more opportunity for cosmic rays to appear however since their locations are random, the stars and other bright objects outshine them as they are a fixed source. Another external particle that would be visible on an image is anything that is on the lense itself. Any dust on the lens would appear as a ring shape on the image. Hence the nickname "dust doughnut". This error is seen in all images taken with that camera as there is no mechanism to remove it. Imperfections of the camera itself would have an effect on the image. This could be anything from dead pixels, to an overspill along a row due to a very intense source overloading a pixel. Images compression type of all images used in this report are "lossless" meaning that information is not lost through the compression process. The alternative is "lossy".

1.1.2. Encke Gap

Saturn's ring system is made up of seven rings. These rings are separated by gaps and divisions[17]. In order of increasing radius they are the D, C, B, A, F, G and E rings. Throughout this paper we focus on the A ring although the F ring is also mentioned.

The Encke Gap is a 325km wide gap in Saturn's outer A ring[17]. The Encke Gap "contains the orbit of the small moon Pan and an array of dusty features composed of particles less than 100 microns across" [8]. The gap was first discovered in 1888 by James Keeler and named after Johann Franz Encke. The dust features referred to in Hedman et al[8] include incomplete ringlets that follow horseshoe and tadpole orbits[15]. In order of increasing radius, there is the inner ringlet, the Pan ringlet, the fourth ringlet and the outer ringlet.

The location of the Encke Gap suggests that it did not arise from resonance with a satellite [15]. Rather, it was probably formed due to a satellite forming in the region and clearing the path as well as maintaining the gap [15]. This satellite is Pan.

Edge Waves Edge waves occur when the massive object moves past the ring particles, attracting them and creating ripples. These waves propagate along the edge of the gap as edge waves and into the ring plane as density waves. The waves along the edge (edge waves) have the highest amplitude and decay along the gap edge (with increasing distance from the moon). This is due to collisions of the wave particles. Dermott's [11] estimate for when these collisions take effect is given by equation 1.1.

Distance to shock front =
$$\frac{3(\Delta a)^2}{2(ae)}$$
 (1.1)

where Δ is the absolute distance between the moon and edge orbital semi-major axes and e is the eccentricity [5]. An approximate wavelength, λ , for these edge waves is given by

$$\lambda = 3\pi \Delta a \tag{1.2}$$

Even if the viewing angle makes it difficult to measure radial variation, the phase angle(incident angle of light from the Sun) can mean that shadows can be cast along the wave itself allowing the peak to be identified as the point beyond where the shadow starts. A variation of optical depth or brightness can also be used to measure the wavelength as these vary with respect to distance and repeat. This allows us to quantise the wavelength of the edge wave that can be seen plainly. Fundamentally, the wave is a repeating pattern. If the pattern is visible, you can measure the length of the motif. This is equivalent to the wavelength however you decide to measure it.

Pan Pan was first discovered by M.R. Showalter using Voyager 2 images by detecting waves along the edge of the Encke gap. These waves suggested that there

was a nearby satellite [15][17].

"The Voyager camera was capable of detecting not resolving the satellite". [15] However, the lack of ability to resolve a satellite does not mean that you cannot prove that it is there. Since it must be following Kepler's laws, we can track it over multiple images. Even if the satellite takes up a single pixel in the image, the pixel that is seen to move in a predictable way, and that is moving at a velocity that would be expected at that radius from the central mass, can lead us to conclude that it is a satellite in orbit and not the result of noise in the image or background star. Pan has a ridge along its equator due to the accretion of particles, from nearby ringlets, on the surface[6]. Pan has a mean radius of 14.1km[17] and semi-major axis of 133584.0km[2].

1.1.3. Keeler Gap

The Keeler Gap is a 37km[10]-wide gap in the outer edge of the A ring (between the Encke gap and the Edge of the A ring). It was first discovered and studied by Voyager in 1991[14]. The edges of the Keeler Gap have waves that are caused by the central object, Daphnis. The observation of these waves led to its discovery as there were waves that were not uniformly present along the edge of the gap. If they were uniformly present then this would suggest that it was related to resonance with one or more of Saturn's moons. The edge waves on the Keeler Gap edge oscillate perpendicular to the plane of Saturn's disc and decay exponentially in the radial direction of Saturn. The peak amplitude is at the location of Daphnis and decays with increasing distance along the Keeler Gap. This why the waves were not uniformly present around the Keeler Gap, leading to the conclusion that a satellite was perturbing the gap.

Like the Encke Gap, the gap appears to have been formed by Daphnis and cleared by it. There are strong resonances associated this region(18:17 with Pandora and 32:31 with Prometheus) but the cores of Daphnis is large enough to have been able to open the gap on its own [15][9].

For Keeler–Daphnis, the radial component is approximately 2.5 km and the $3\pi\Delta a$ is about 165 km.

1.1.4. Daphnis

Discovery Prior to direct observation of Daphnis, waves along the edge of the Keeler Gap suggested that there may be an object perturbing the gap as well as

forming it [17].

Effect on Keeler Gap The waves on the inner and the outer edge are not side by side. The inner edge wave is ahead of Daphnis and the outer edge wave follows Daphnis This was because Daphnis gravitationally attracts the particles at the Keeler Gap edge. Since R^3 α T^2 , the inner edge ($R < R_{\text{Daphnis}}$) is moving faster than Daphnis and outer edge ($R > R_{\text{Daphnis}}$) is moving slower than Daphnis. This means that inner edge wave leads and the outer edge wave trails. This is also seen in propeller moonlets embedded in the rings. The same process but on a smaller scale. It has an inclination of $0.0036(13)^{\circ}$ which is much greater than Pan which has an inclination of $0.0001(4)^{\circ}[2]$. This also means that the waves are more prominent, especially near equinox. At this time, the angle of the incident sunlight is low therefore long shadows are cast over the A ring, making this the best time for collecting information on the waves. The length of the shadow is proportional to the amplitude of the wave.

Properties Daphnis has a radius of 3.8km and has a semi-major axis 136,500km[17]. In Fig. 1.1a and Fig. 1.1b, Daphnis has an equatorial ridge but also seems to have further ridges. This indicates that Daphnis may have been oriented differently, as these appear to be previous equatorial ridges.

Behaviour Since we now have many confirmed observations of Daphnis, we should be able to calculate an accurate value for the mean motion. However the mean motion appears to be changing. According to Jacobson [3] the mean motion appears to have changed twice, giving us 3 values for the mean motion. The equatorial elements for Daphnis calculated by Jacobson are given in Table 1.1. In this report we aim to look at possible explanations for this variation of orbital elements.

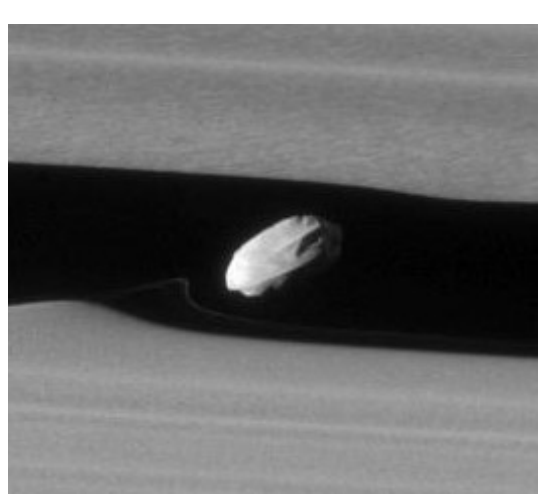
This may be connected to the 4 ridge lines that can be see in Fig. 1.1b.

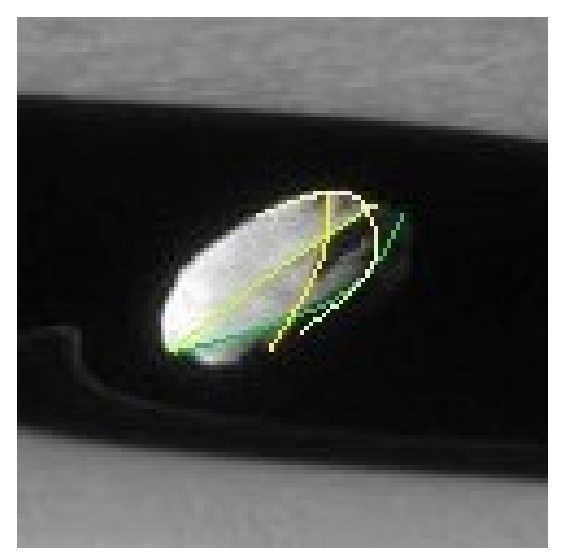
1.1.5. Software

Caviar is an image processing and astrometry software used in order to create a QMPF (QM Pointing File). It was created to view, modify and manipulate the raw images from Cassini however it can be used to view other raw images too[7]. Caviar uses the IDL programming language. To use it, open an image and set which planet is of interest by loading feature as shown in the screenshot Fig. 1.2.

Table 1.1.: Daphnis Planetocentric Equatorial Elements Credit: Jacobson JPL/Caltech[3]

Element	Orbit A	Orbit B	Orbit C
Epoch JD	2451545.0	2451545.0	2451545.0
a (km)	136505.539 ± 0.045	136505.668 ± 0.05	136505.608 ± 0.050
$e (\times 10^3)$	0.0192 ± 0.0055	0.0119 ± 0.0078	0.0210 ± 0.0189
ϖ (deg)	73.3 ± 18.7	263.8 ± 50.0	265.2 ± 55.0
$\lambda \text{ (deg)}$	153.5702 ± 0.0056	156.8313 ± 0.0227	154.6459 ± 0.2889
i (deg)	0.0016 ± 0.0006	0.0043 ± 0.0012	0.0020 ± 0.0022
Ω (deg)	104.7 ± 20.7	115.2 ± 9.9	178.1 ± 56.2
$\frac{d\lambda}{dt}$ (deg/day)	605.9791559 ± 0.000002	605.9783385 ± 0.000005	605.9787247 ± 0.000048
$\dot{\vec{\varpi}}$ (deg/day)	2.969000 ± 0.000297	2.969004 ± 0.000297	2.969003 ± 0.000297
$\dot{\Omega} (\deg/\deg)$	-2.954598 ± 0.000295	-2.954599 ± 0.000295	-2.954597 ± 0.000295





(a) Closeup of Daphnis

(b) Lines are along the four ridge ridges

Figure 1.1.: Daphnis close up, Image Name = N1863267232; Target = Daphnis; Image Mid-Time = 2017-016 13:06:18.761 UTC; Exposure = 460s; Radial Resolution = 0.3461. Image Credit: NASA/JPL-Caltech/Space Science Institute

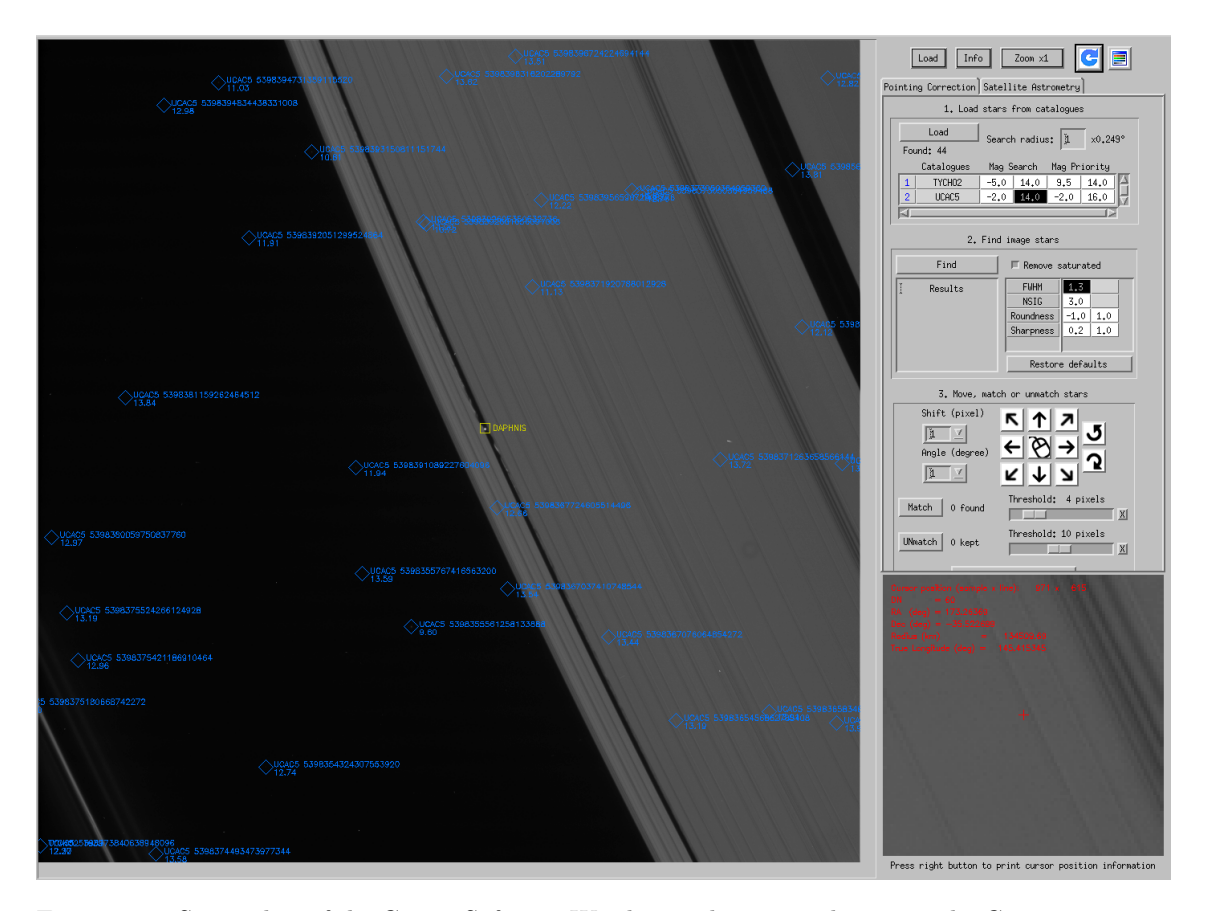


Figure 1.2.: Screenshot of the Caviar Software Window with a pointed image. The Cassini image in the example is N1612038605. Later in this report it is labelled as Image G. For image details, see Table 3.1. Image Credit: NASA/JPL-Caltech/Space Science Institute

First "load" the locations of the stars. The default maximum magnitude is 11. This means that the locations of all stars brighter than 11 will be indicated with a blue diamond and tagged with their name/number and magnitude. This will make it immediately obvious if the image is pointed. We point the image because this orients it, shifting the template so that stars observed are accurately labelled and allows us to take accurate measurements. If this image has already been pointed, we can load the associated pointing file. Loading a pointing file seemingly adjusts the predicted location of the stars but this is due to the fact that by default, Caviar is using where Cassini thought it was at the time to predict which stars would be visible in this image. To do this, Caviar uses information from the TYCHO2 and UCAC5 star catalogues. Pointing has no effect on the right ascension (RA) and declination(Dec) associated with each pixel in the image. Caviar is regularly updated to ensure that any new stars and catalogues are added and orbital elements are up to date. If there is no QMPF file for this image then you can create one by

adjusting the default predictions of the stars such that they line up with visible stars in the image. This can be checked against the "Find stars" feature. This searches the image for any collections of bright points that could be a star, with adjustable thresholds. Then you "Match stars" and compare with your observed locations and what the "Find Stars" feature found. It is common for the "Find stars" feature to confuse Saturn's disc with a star due to its brightness. If a star is supposed to be located in that position, the brightness of the disc is mistaken for a star that is not actually visible. These false positives can be deselected. We can save this a new QMPF file for future use. Once you have a pointed image, measurements can be taken using the cursor to select a pixel. The zoom feature can magnify the image up to 10 times. At this magnification, individual pixels are easy to select and each pixel is practically unmissable therefore reducing the error to the resolution of the image itself. Caviar also allows you to adjust the image itself such as stretching it (ignoring limited regions of the light curve), reverse colours and many other features as shown in the screenshot. We only used the two features mentioned in order focus on finer detail. Switching between positive and negative images can help with seeing individual pixels that differ from their surroundings as they would have the greatest change in brightness, measured as Digital Number (DN). The window at the bottom right corner of Fig. 1.2 also gives information about that particular pixel. If the image is not pointed it will give the line x sample (coordinates of the pixel within the image), the DN, the Right Ascension (RA) and Declination (Dec). Once the image has been pointed we can also see the radius from the centre of the planet (always Saturn throughout this paper) and the True Longitude (the angle measured along the plane of the disc). This information is printed to the console when clicking on a target pixel.

2. Method

2.1. Strategies, selection

In order to be gain a full understanding of the images taken by Cassini, the natural option would be to look at all the images. Cassini took 395,927 images during its mission[12]. Due to constraints, it was not possible or efficient to go through every single image individually. This meant having to strategise to efficiently filter which images were relevant to this project while minimising the amount spent checking individual images.

2.1.1. Criteria

The initial criteria for relevance to this project were as follows. Visible light images (CL1 and CL2 filters), Saturn's A ring in the field of view, and the higher resolution the better. Since we only wanted to view visible spectrum images, this leaves us with two options: Narrow and Wide angle images taken by Cassini's Imaging Science Subsystem (ISS). The OPUS software is a tool used to search through and analyse image sets from NASA outer planetary missions[16]. Using OPUS, we were able to filter images based on our criteria, to select higher resolution images and specify targets. This further reduced the amount of searching required. The list of criteria grew as we encountered obstacles such as highest resolution images being too close to point accurately. Another obstacle faced was Saturn's shadow hiding the rings.

2.1.2. Daphnis targeted images

We first searched for images that had Daphnis as the target. There are 735 Daphnis targeted images. This would guarantee that the Keeler Gap was in view but it would mean that a corotating object at Lagrange Point 3 (located at 180° from Daphnis) or in a tadpole orbit would permanently out of frame. In order to view the rest of the ring (the parts that are not disturbed by Daphnis), we searched for images in which Pan or Prometheus were the target.

2.1.3. Indirect observation

Since Pan and Prometheus have similar orbital radii to Daphnis, we could indirectly view the rest of the Keeler gap. FMOVIE and F streamer channel images were useful to give a more continuous view of the ring. These types of images are part of a series of images the target the F ring region. FMOVIEs track a particular point of interest or region as it orbits Saturn (usually Prometheus). F streamer channel images stay fixed and wait for the objects to pass through the field of view. Both of these types of image sequences give a continuous view of the F ring but they also give us a near continuous of Keeler Gap as it is often visible in the images. Daphnis and the Keeler Gap have a smaller orbital radius than the F ring or Prometheus. Therefore, if images are taken perfectly in sequence for the F ring (regular intervals such that there are no gaps or overlaps) the images of the Keeler Gap will not be. This is an acceptable compromise since we can now view the rest of the Keeler Gap where Daphnis is not present. This significantly lowered the probability of missing an object or other localised feature.

2.2. Brute Force Searching

Some pictures were targeted at "rocks" or "rings" but happen to also capture the Keeler Gap or even Daphnis The next step was manually to check each image and set aside anything unusual or of note for further analysis. This step included checking which images did not have pointing files associated with them. This meant that they could not be included in mosaics until they were pointed. A mosaic is the image produced by stitching together smaller images, using their pointing files so that each image can be re-projected and placed according to the range true longitude and radius. The result is a type of panoramic image known as mosaic.

2.3. Possible avenues

While conducting the discovery phase of my project we made note of particular images of interest and decided to use these to define possible avenues of further investigation. One aspect we wanted to confirm was whether the Keeler Gap edge waves dissipated uniformly on either side of Daphnis and whether it was consistent. This is a difficult task due to the variation in the geometry between images. This could be addressed by using the original images and manually taking measurements of Digital Number (DN) along a ring plotted at radius (using the ring tool as part of

the Caviar software). Despite the variation in brightness and geometry of the images, the oscillations of the DN with respect to the true longitude can be analysed to find the rate of decay. The graph plotted for the outer edge and the inner edge can then be compared. In future this can be simplified by using reprojections of individual images and creating a tool to automatically plot all the DN values of a selected row in the image.

2.4. Orbit Predictions

Satellites in orbit move in a predicable way. In order to make a prediction, we need to know where the satellite was at a certain time, what it's mean motion is and what the new time is. Whenever an anomalous pixel or bright region is observed, we can check if it is in orbit of Saturn by seeing if it matches the predicted behaviour. To accelerate the process, we wrote a formula in Microsoft Excel spreadsheet to automatically make the calculation when values for each variable are given. To test the accuracy of these calculations, we used 9 example images (across approximately 33 days). Each image was known to contain Daphnis. The actual location of Daphnis was then compared to the predicted location for each image to give a value for the uncertainty and greatest uncertainty was 0.1571784° of true longitude. The results can be found in Table 2.1. This is significant as it indicated the error associated with applying these calculations to other objects and therefore aids in calculating a mean motion error for a potential object. The error, as expected, increased over time and varied depending on the resolution of the image.

2.4.1. The Calculation

By considering that the mean motion, n, of Daphnis is 605.979162(5) °/day[2]. We decided to convert degrees/day to degree/s since the images integer time intervals were easier to calculate. We can convert the mean motion into degrees/second by dividing by (24 * 60 * 60), giving us the factor 0.00701364771°/s. This factor was substituted in to equation 2.1 as a value for n.

$$\theta_{\text{final}} = ((\Delta t \times n) + \theta_{\text{initial}}) \mod 360$$
 (2.1)

where Δt is the change in time from when image N1612090564 was taken, to the time that the new image was taken. θ is the true longitude. The results can be found in Table 2.1.

Table 2.1.: Testing Excel calculations on targeted images of Daphnis. These calculations are used to predict the location of an object after time interval Δt

\mid Image Name \mid Δ t (days) \mid Δ t (s)	Δ t (days)	Δ t (s)	True Long.	True Long.	Obs-Predict (°)
			(Predicted) (°)	(Observed) (°)	
N1610354958	20.087894	-1735594	216.199647	216.194215	0.005432088
N1611809569	3.2522338	-280993	338.259042	338.242083	-0.016958536
N1612038605	0.6013773	-51959	144.622898	144.620858	-0.002039568
N1612038648	0.6008796	-51916	144.924484	144.924574	0.000089568
N1612090521	0.0004977	-43	148.743447	148.741857	-0.001590136
N1612090564	0	0	149.045034	149.045034	0
N1613936508 21.3649306	21.3649306	1845930	135.748287	135.750746	0.00245936
N1614668948 29.8421875	29.8421875	2578365	232.78956	232.788545	-0.0010452
N1614963580 33.2522569	33.2522569	2872995	139.22067	139.216524	-0.00414576
N1733157232 1401.22517	1401.22517	121065855	22.336823	21.669177	-0.66764604
N1736967706 1445.3276 124876305	1445.3276	124876305	107.491845	106.809752	-0.68209264

2.5. Calculated Constraints

If there is another object present in the Keeler Gap. It would likely be in a horseshoe or tadpole orbit. These types of orbits would affect the orbital radius and the mean motion of Daphnis as shown in Fig. 2.1 and could explain the variation in Daphnis' orbit as highlighted by Jacobson [3]. It is simplest to assume a singular object although it is possible that there are several. For the purposes of these calculations, we assume a single object in the Keeler Gap aside from Daphnis. We can calculate constraints given that the width of the Keeler Gap is limited and that mass of Daphnis is known. The Keeler Gap is approximately 37km wide [10]. This limits the variation in orbital radius of any object to $|\Delta a_{\text{Object}}| < 18.5 \text{ km}$. There are 2 recent values for the mass of Daphnis. They are $7.7\pm1.5\times10^{16}$ kg[4] and $8.4\pm1.2\times10^{16}$ kg[9]. The density of Daphnis is $340 \pm 260 \text{kg/}m^2$ [10]. These values are presented in Table 2.2. We assume that another object in the Keeler Gap would have equivalent density (as is the case with Janus and Epimetheus). For the variation of Daphnis' orbital radius, $\Delta a_{\text{Daphnis}}$, we look the three orbits calculated by Jacobson[3] and take the two with the greatest difference as this is a boundary for our constraint calculations. We substitute these values in equation 2.2 and the results are given in Table 2.5.

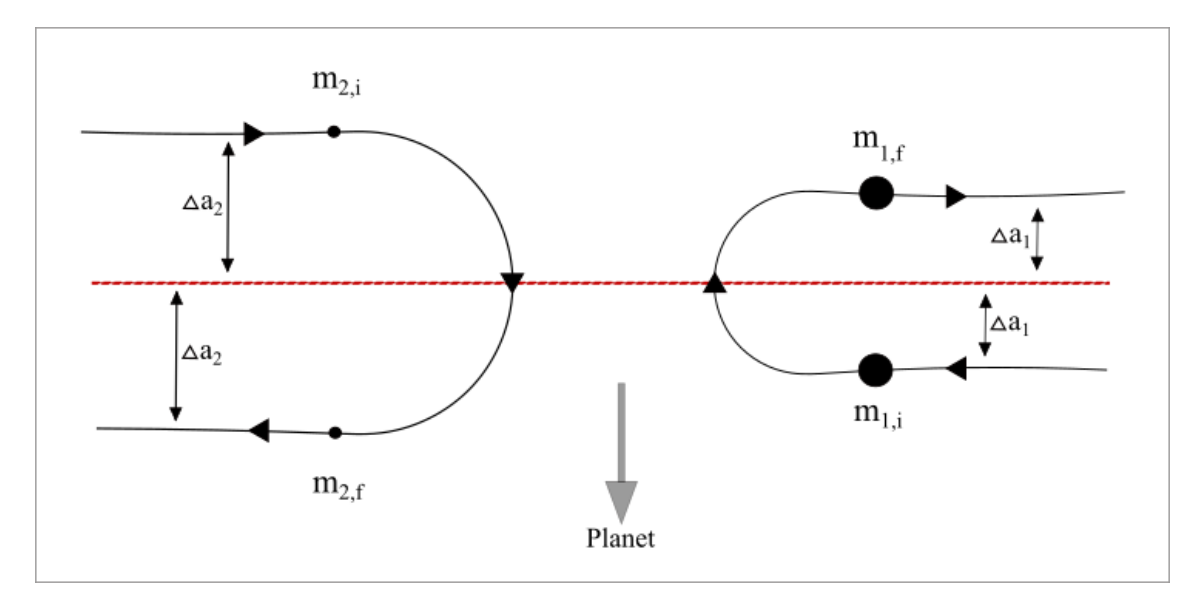


Figure 2.1.: This diagram shows a close up of the change in orbital radius, Δa , of two masses, m_1 and m_2 , as they approach each other in their orbits. This is from a co-orating perspective. The initial and final locations are indicated by the subscript "i" and "f" respectively. The dotted line indicates a midpoint in the orbit.

$$mass_{\text{Object}} \sim mass_{\text{Daphnis}} \times \frac{\Delta a_{\text{Daphnis}}}{\Delta a_{\text{Object}}}$$
 (2.2)

Table 2.2.: Mass and Radius values for Daphnis according to Thomas[4] and Porco[9]

Source	Mass (Daphnis) (kg)	Radius (Daphnis) (m)
Thomas[4]	$7.7 \pm 1.5 \times 10^{13}$	3800 ± 800
Porco[9]	$8.4 \pm 1.2 \times 10^{13}$	3900 ± 800

Source	Mass (Object) (kg)	Radius (Object) (m)
Thomas[4]	$2.7 \pm 0.5 \times 10^{11}$	570 ± 360
Porco[9]	$2.9 \pm 0.4 \times 10^{11}$	590 ± 360

The calculated value for the radius of the potential object is a lower bound.

2.6. Points of Interest

After we successfully tested the Daphnis' orbit predictions in Section. 2.4, we can apply it to anything of interest to see whether it was worth investigating further. Using the equation 2.3 we calculate that the orbital period of Daphnis is 51328.4977 seconds.

$$T = \frac{360}{n} \tag{2.3}$$

where n is the mean motion and T is the orbital period. A single image cannot give us the mean motion. We would need a second image in order to calculate the mean motion, given the change in true longitude during the elapsed time.

$$\theta_2 = \theta_1 * \frac{dt}{T} \tag{2.4}$$

where

$$\theta_2 = \theta_1 + d\theta. \tag{2.5}$$

In this case, $d\theta$ is the change in true longitude and dt is the elapsed time between the images. We can also use Daphnis' mean motion and time period to approximate how many orbits an object could have made in the time, dt. Taking note of the True Longitude and the mid-time of each image, we calculate the mean motion in degrees per second using equation 2.6 and equation 2.7.

$$n_{\text{object}} = \frac{(360 \times orbits) + d\theta}{dt} \tag{2.6}$$

where

orbits =
$$\frac{dt}{T_{\text{Daphnis}}}$$
 (2.7)

We then convert the value back to degrees per day as this is the standard form. Given that equation 2.7 relies on a mean motion value from Daphnis, the mean motion of the object (equation 2.6) will tend towards the mean motion of Daphnis at greater time intervals. However this value will be increasingly inaccurate. As with the Daphnis prediction calculations in section 2.4, we used these equations as Excel formulae to accelerate the process of checking the mean motions of potential objects.

3. Results

3.1. Bright Dots and their Mean Motions

There were many anomalous points found during the investigation. The list of possible candidates can be found in Table 3.1

3.1.1. Candidate Images

Image C Fig. 3.19 shows a similar sized object in the Keeler Gap, however it is brighter (DN = 869 as opposed to DN = 95). This image was taken 70 days earlier than Fig. 3.3b. Left in image C is the direction of decreasing radius.

Image D Fig. 3.2 we see that using the "find stars" feature on caviar, the bright object in the gap has been marked with a purple diamond. For image details, see Table 3.1.

Image E In Fig. 3.3a we see the window of the Caviar software with the full image and (since this image was been pointed) blue diamonds indicate the location of stars up to a magnitude of 11.0, as predicted by TYCHO2 and UCAC5. Due to the longer exposure of these images, background stars are seen as streaks of light of approximately uniform length. In the middle of the circle in the top right corner we

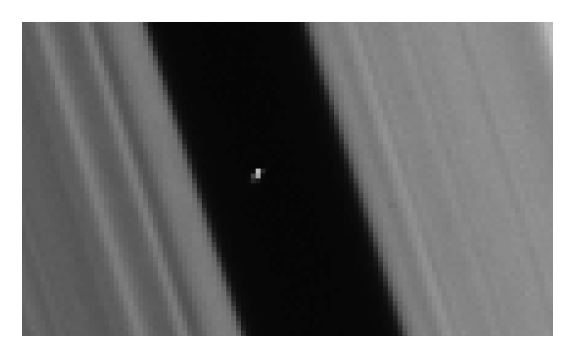


Figure 3.1.: Image C (Cropped and magnified); For image details, see Table 3.1. Image Credit: NASA/JPL-Caltech/Space Science Institute

Table 3.1.: Points of interest and their locations in each image

Label	Label Image Name	Target	Image Mid-Time (UTC) Exposure Radial Resolution	Exposure	Radial Resolution
				(ms)	$(\mathrm{km/px})$
A	$N1495305562^{1}$	Saturn (Rings)	2005-140 18:12:05.912	100	12.18283
В	N1493614056	Saturn (Rings)	2005-121 04:20:30.803	180	7.60954
C	N1584974874	Saturn (Rings)	2008-083 14:10:55.843	089	1.18092
О	N1585782249	Saturn (Rings)	2008-092 22:27:04.967	1000	1.486
田	N1591065387	Saturn (Rings)	2008-154 01:58:45.690	1000	1.5842
ഥ	N1591068064	Saturn (Rings)	2008-154 02:43:22.761	820	2.07191
ŭ	N1612038605	Daphnis (Rocks)	2009-030 19:49:54.640	089	6.24372
Н	N1612090521	Daphnis (Rocks)	2009-031 10:15:10.270	089	5.39245
Н	N1612899640	Prometheus (Rings)	2009-040 19:00:23.091	1500	9.85682
ſ	N1612909228	Prometheus (Rings)	2009-040 21:40:11.023	1500	6.71619
K	N1614963580	Daphnis (Rocks)	2009-064 16:19:08.840	089	6.82189
П	N1742284130	Prometheus (Rings)	2013-077 06:54:09.731	1000	9.41869
M	N1743631128	Saturn (Prometheus)	2013-092 21:03:58.989	1000	2.98055
			(6)	(0)	

Orbital Radius
(km)
136490.84 ± 6.65
136482.01 ± 7.685
136499.99 ± 0.74
136491.48 ± 0.44
136490.97 ± 2.465
136506.46 ± 1.005
136486.71 ± 12.235
136493.06 ± 6.655
136497.86 ± 6.12
136476.13 ± 7.89
136500.12 ± 6.55
136504.17 ± 12.205
136508.22 ± 2.67

contribution from N.J. Cooper (personal communication)

$605.977034 \pm 75871.87076$	127319701	N1742284130	N1614963580	K-L
$605.8900615 \pm 31378.82923$	97454008	N1591068064	N1493614056	B-F
$605.8333711 \pm 4537.909728$	27063731	N1612038605	N1584974874	C-G
$604.6584275 \pm 4402.533166$	26256356	N1612038605	N1585782249	D-G
$604.1929567 \pm 3938.810081$	21834253	N1612090521	N1591065387	E-H
$604.4682521 \pm 5193.905827$	21830576	N1591068064	N1612099640	I-H
$604.3213133 \pm 3233.297768$	21022457	N1591068064	N1612090521	H-F
$604.1909712 \pm 4220.042795$	20973218	N1612038605	N1591065387	E-G
$605.938349 \pm 1609.147635$	6093190	N1591068064	N1584974874	C-F
$606.3821609 \pm 1072.6944$	6090513	N1591065387	N1584974874	C-E
$600.118058 \pm 1233.185629$	5285815	N1591068064	N1585782249	D-F
600.6267446 ± 767.8348	5283138	N1591065387	N1585782249	D-E
$595.2431504 \pm 857.8708567$	2873039	N1614963580	N1612090521	H-K
$605.2319832 \pm 614.4419546$	2054352	N1614963580	N1612909228	J-K
$594.0555426 \pm 661.4384278$	1691506	N1493614056	N1495305562	A-B
$583.0463992 \pm 1178.966474$	1346989	N1743631128	N1742284130	L-M
$571.9682596 \pm 244.6032208$	861028	N1612099640	N1612038605	G-I
$569.8484177 \pm 218.6303506$	809113	N1612099640	N1612090521	H-I
$605.5184465 \pm 205.3882713$	807375	N1585782249	N1584974874	C-D
$605.006719 \pm 16.68948037$	51916	N1612090521	N1612038605	G-H
$597.151419 \pm 2.595559907$	9588	N1612909228	N1612899640	I-J
$-403.7897384 \pm 0.415031971$	2677	N1591068064	N1591065387	H-H
Mean motion, $n (\deg/\deg)$	Time Interval (s)	${\rm Image}\ 2$	Image 1	Labels

Table 3.2.: Mean Motion as calculated between 2 images

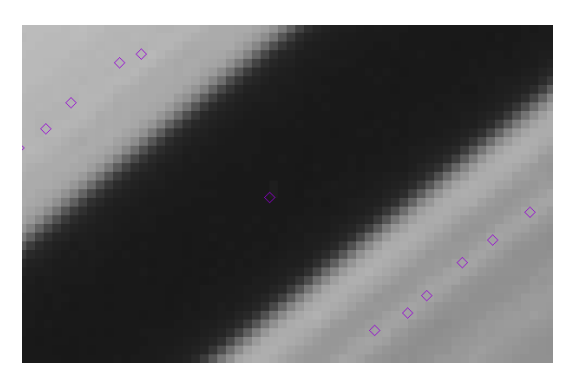


Figure 3.2.: Image D (cropped); For image details, see Table 3.1. Image Credit: NASA/JPL-Caltech/Space Science Institute

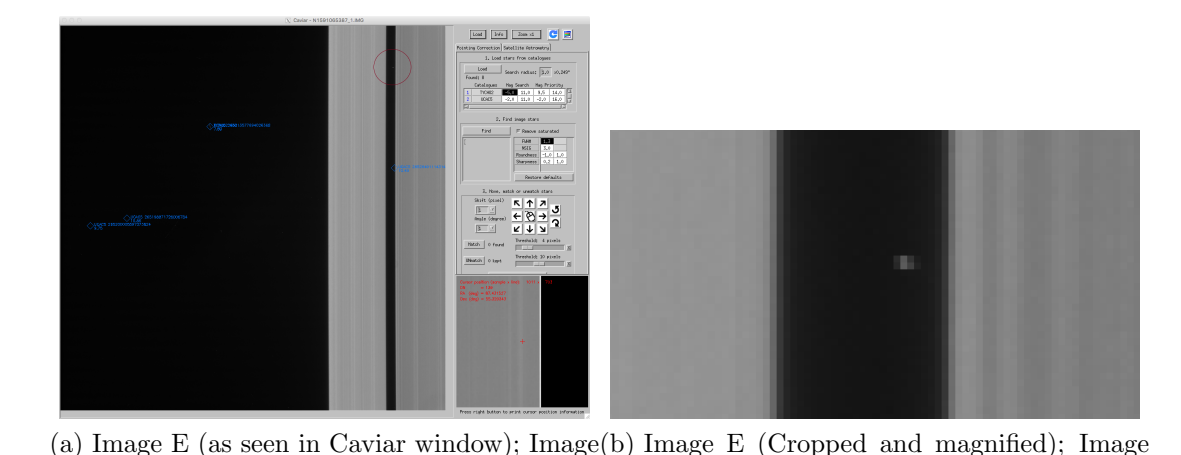


Figure 3.3.: For image details, see Table 3.1.

Institute

Credit: NASA/JPL-Caltech/Space Science

Credit: NASA/JPL-Caltech/Space Science

Institute

see a brighter region of pixels. Fig. 3.3b is a close up of this region. We can see that there are approximately 8 pixels that are brighter than the gap itself and of similar brightness to the disc itself in this region. For image details, see Table 3.1.

Image F There are 4 distinctly brighter pixels at left of centre of the image. The left direction in the image is the same direction as towards Saturn.

Image G In Fig. 3.5a, we see arrow 1 indicating Daphnis with its waves on either side of the gap. The amplitude of these waves decay with increasing distance from Daphnis. At arrow 2 we see a collection of bright pixels that is within the gap. These pixels appear to be slightly brighter than the disc near the object. This is also true for Daphnis relative to the nearby disc and the waves. In Fig. 3.5b, we no longer see Daphnis (as it has been cropped) but we the image is centred on 4 brighter

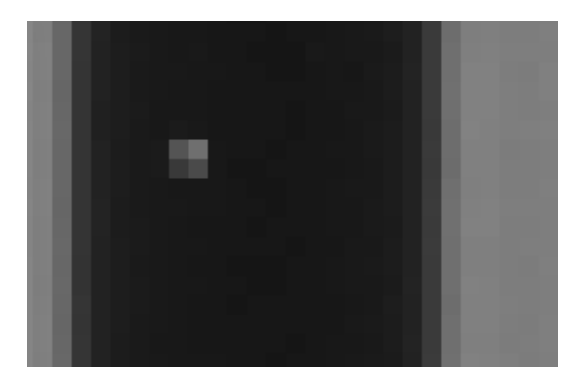


Figure 3.4.: Image F (cropped); For image details, see Table 3.1. Image Credit: NASA/JPL-Caltech/Space Science Institute

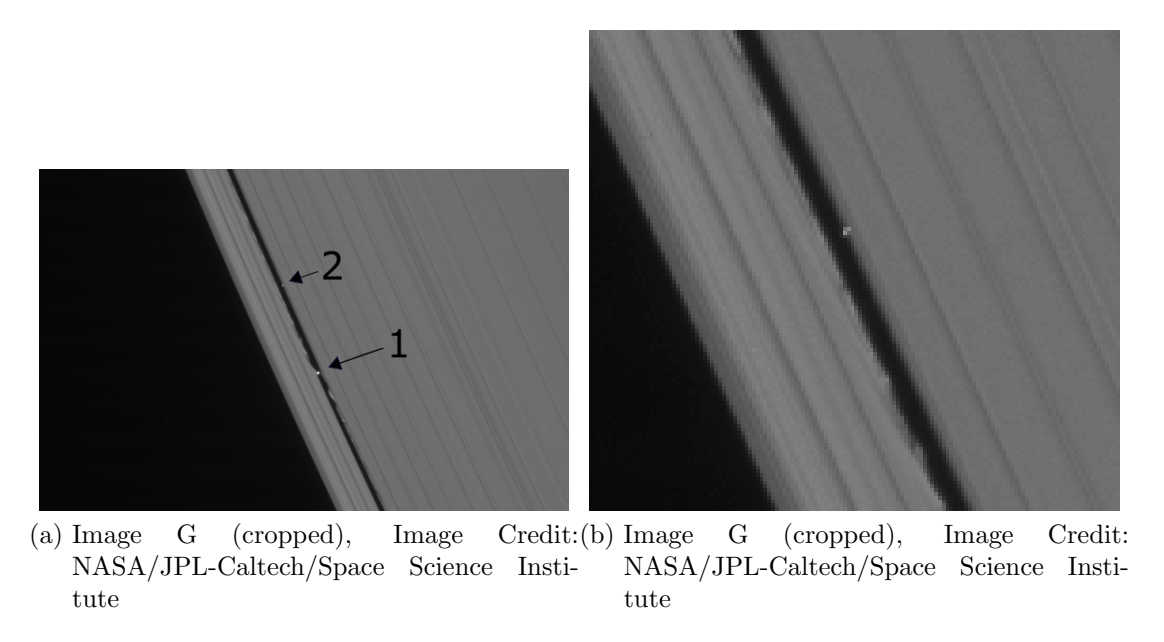
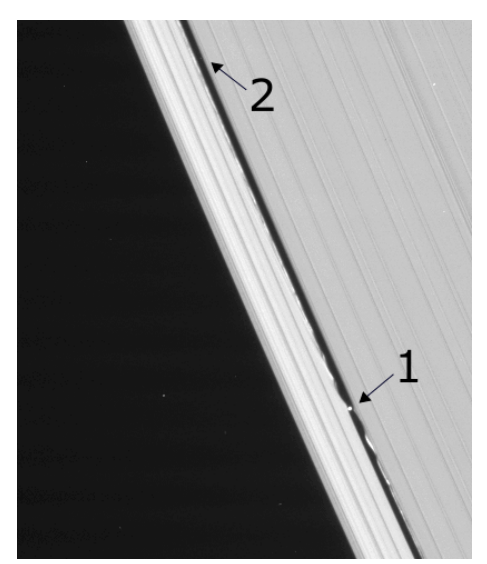


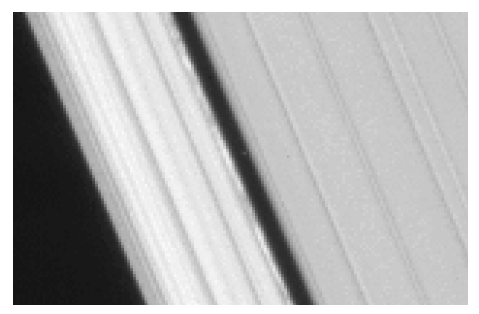
Figure 3.5.: For image details, see Table 3.1.

pixels in the Keeler Gap. At first glance it appears as if it is embedded in the edge of the Keeler Gap, this is not the case as it is sharper and such and object would be disrupted if it were there. It is also worth noting that it's brightness changes in line with the Keeler Gap. Saturn's disc is not opaque meaning something behind it (relative to the Cassini spacecraft) could shine through.

Image H Image H; Daphnis and the waves caused by it can be seen in image (Fig. 3.6a). Daphnis has be indicated by arrow number 1. The bright dot of interest is indicated by arrow 2. Fig. 3.6b is and cropped version of 3.6a in which there is a brighter region of pixels within the Keeler Gap. This image was taken \sim one Daphnis orbit later than Image G in Fig. 3.5a.



(a) Image H (cropped; includes Daphnis), Image Credit: NASA/JPL-Caltech/Space Science Institute



(b) Image H (cropped), Image Credit: NASA/JPL-Caltech/Space Science Institute

Figure 3.6.: For image details, see Table 3.1.



Figure 3.7.: Image I (cropped); For image details, see Table 3.1. Image Credit: NASA/JPL-Caltech/Space Science Institute

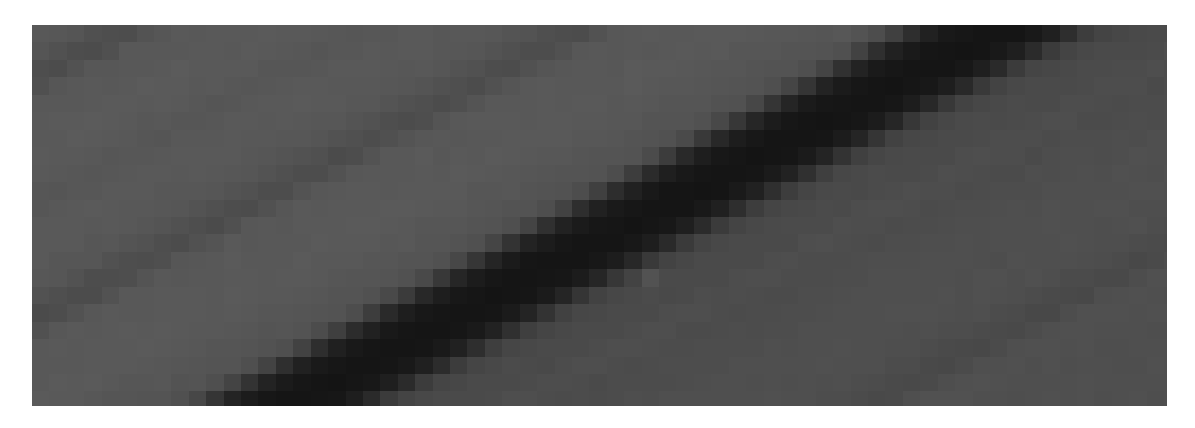


Figure 3.8.: Image J (cropped); For image details, see Table 3.1. Image Credit: NASA/JPL-Caltech/Space Science Institute

Image I In Fig. 3.7 at that centre, we see a bright couple of pixels with a slight blurring of the Keeler Gap edge.

Image J In Fig. 3.8 the dot appears to be near, or behind the Keeler Gap edge. Despite this it is worth noting as Daphnis' orbit is inclined, it is possible that another object in the gap would also have an inclined orbit.

We could assume that any object in the Keeler Gap should have approximately the same mean motion as Daphnis. Using the same method as previously described we could calculate where it would be at the time that a different image was taken. With a calculated mean motion, it is also possible to feed this value into the same equations as for Daphnis to determine whether it should be visible in subsequent images. If it is visible in subsequent images, we can use any error to fine tune the value of the mean motion.

3.1.2. Possible background star

Some of the images, we have separated out. They are consecutive images taken as part of an FMOVIE. In each of them have a bright dot that appears to be in the Keeler Gap. The apparent locations of these bright dots are given in Table 3.4. These locations are only apparent as the assumption is made that everything is in the plane of Saturn's disc. However when we calculate the mean motion of the object (results in Table 3.5) we see that this mean motion does correspond with what we would expect from an object in the Keeler Gap. In addition, in the 4th image, the object appears to go behind the a ring disc. We then look to the change in Right Ascension (RA) and Declination (Dec) See Table 3.4. It is a near constant value but not exactly. These are pointed images but any pointing errors would contribute to a change in RA and Dec. However even taking that into consideration. A background star should not move 33 arcseconds in 4.5 hours. The rate of variation of the RA and Dec also suggests that is it not moving in the background. Rather it is either approaching or receding. We then look to the cursor position (sample x line). The first two are identical (320 x 144). The final one is different (891 x 53). Anomalies at the same pixel are usually attributed to imperfections in the camera e.g. a dead pixel. A dead pixel appears dark. A stuck pixel could appear bright but we also have to take into account that these images were not taken long after during an FMOVIE (in which the field of view doesn't change much). Therefore, possibilities include (from most likely to least likely): a stuck pixel that has a coincidental encounter with an unlabeled background star in the final image; a background star that is in a seemingly near fixed position as FMOVIE sequential images have approximately the name viewing angle; one of the planets in our solar system; a moon orbiting Saturn in a highly inclined, unusual orbit. More calculations need to be made to confirm that it is not a planet or distant moon. These are topics for future research as it is almost certainly not related to the Keeler Gap.

3.2. Propeller

One of the images that has a bright dot, also appears to contain a propeller. This can be determined by the two arms that can be seen in Fig. 3.11. The arms extend approximately equal distance in both directions, with rotational symmetry. It is located by the outer edge of the Keeler Gap in the disc. The details on the N1591068064 (the image with the propeller) can be found in section 3.1

Table 3.3.: Details for images containing the bright object (possible background star)

					2	β	Q		Lal
<u>_</u>	β	α	L_{ε}		Z	Z	Z		bel Ir
			ւbel R		159644'	159643	159643		Label Image Name
166	166	166	ight A		7770	1845	1600		ame
166.17752	166.10877	166.04153	Label Right Ascension(°) Declination(°)	Table 3	N1596447770 Saturn (Rings)	N1596431845 Saturn (Rings)	N1596431600 Saturn (Rings		Taı
			$\operatorname{n}(°) \mid \Gamma$	8.4.: Loca	(Rings)	(Rings)	(Rings)		Target
-49.899362	-49.816343	-49.729655	eclinat)	ations of	_) 200) 200		Ima
)362	343)655	$\operatorname{ion}(°) \mid$	bright o)8-216 ()8-216 ()8-216 (ge Mid-
13649_{2}	13649	13648	Ra	Table 3.4.: Locations of bright object (possible background star	2008-216 09:41:30.240	2008-216 04:39:05.752	2008-216 04:35:01.354		Image Mid-Time (UTC) Exposure (ms)
$136494.86 \pm 3.805 \mid 217.641591$	136497.22 ± 5.03	136489.36 ± 5.04	Radius(km)	ossible b	0.240	5.752	1.354		UTC)
3.805	5.03	5.04	1) (ackgrou					Expos
217.641	216.58	216.57812	True Lo	nd star)	680	680	680		sure (m
	$4561 \pm$		Longit					Re	$\frac{\mathbf{s}}{\mathbf{s}}$
± 0.0011175	216.584561 ± 0.00850	± 0.001609	ngitude (°)		4.77	5.57622	5.5892	Resolution (km/px)	Ra
75)1	0			4.77713	$^{7}622$	892	$_{1} (km/_{1})$	Radial
								px	

Table 3.5.: Mean motions of the object between images

Image 1 | Image 9 | Mean Motion (dec/day) |

$5.682368237 \pm 0.014568312$	γ	α
$5.734844082 \pm 0.018473595$	Z	β
$2.271438367 \pm 1.200783673$	β	α
Mean Motion (deg/day)	Image 2	Image 1

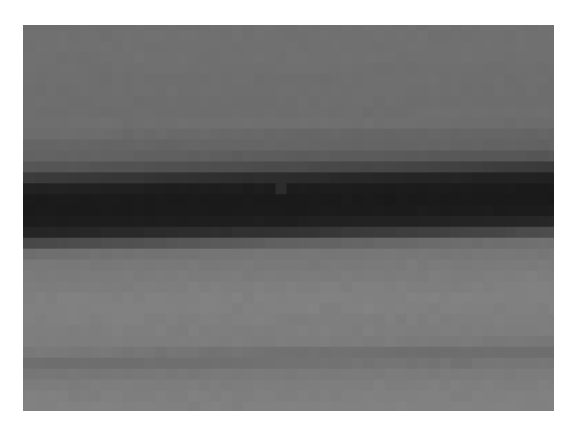


Figure 3.9.: Image α , Image Credit: NASA/JPL-Caltech/Space Science Institute

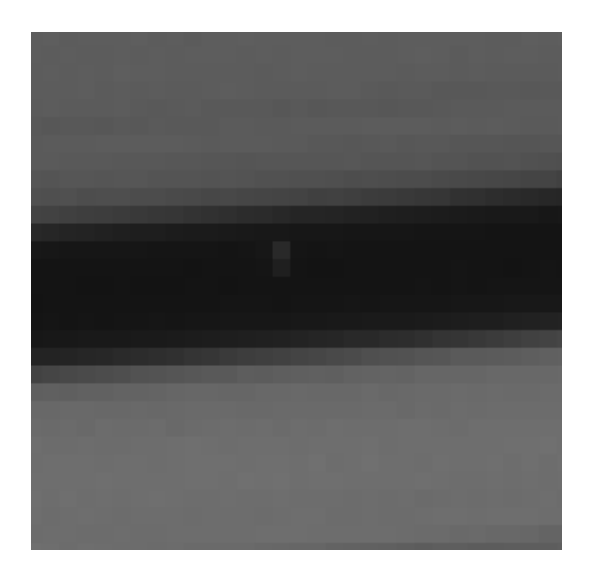


Figure 3.10.: Image $\gamma,$ Image Credit: NASA/JPL-Caltech/Space Science Institute

3.3. Waves at the Keeler Gap edge

While searching through the images that had the Keeler Gap in view (radius of 136,000-137,000km in view) we noticed an untargeted image of Daphnis. This image clearly showed the waves on each edge of the Keeler Gap but it also seemed to show a few further waves on the outer edge of the Keeler Gap. In order to check that these waves were not part of the natural decay of the edge waves, we decided to measure the DN value along a curve plotted, using Caviar software. We used these values and plotted a graph of DN vs True Longitude. This can be be seen in Fig. 3.12, Fig. 3.13 and Fig. 3.14. We also applied this method to a Daphnis targeted image N1612090521 as seen in Fig. 3.6a and Fig. 3.6b. This is the image shown in the Caviar Software example.

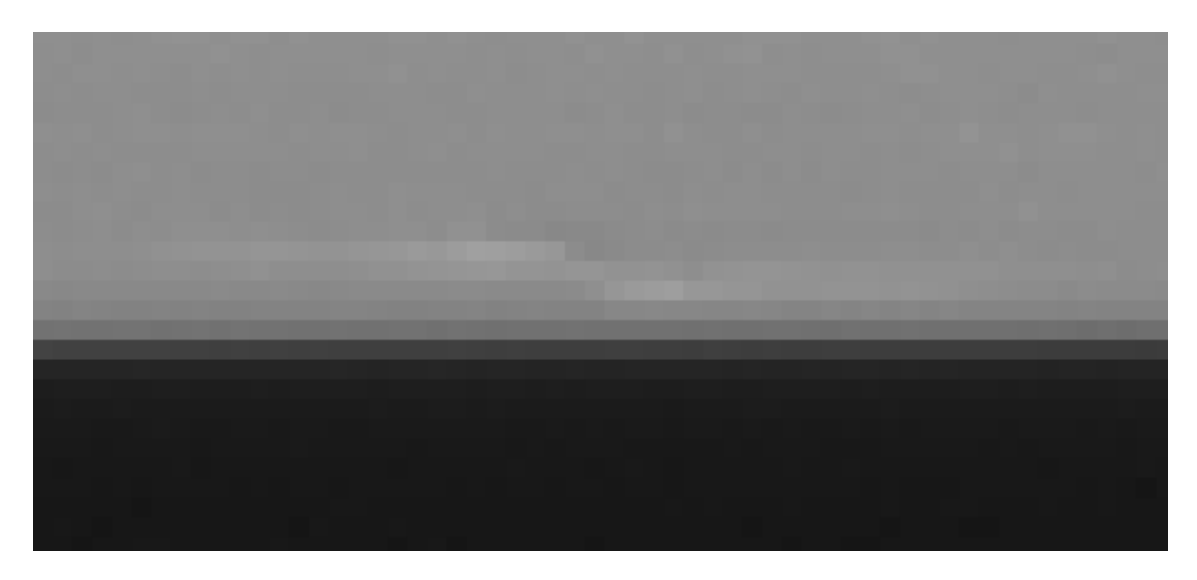
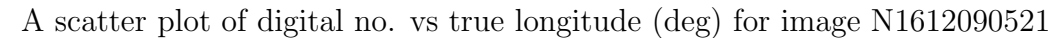
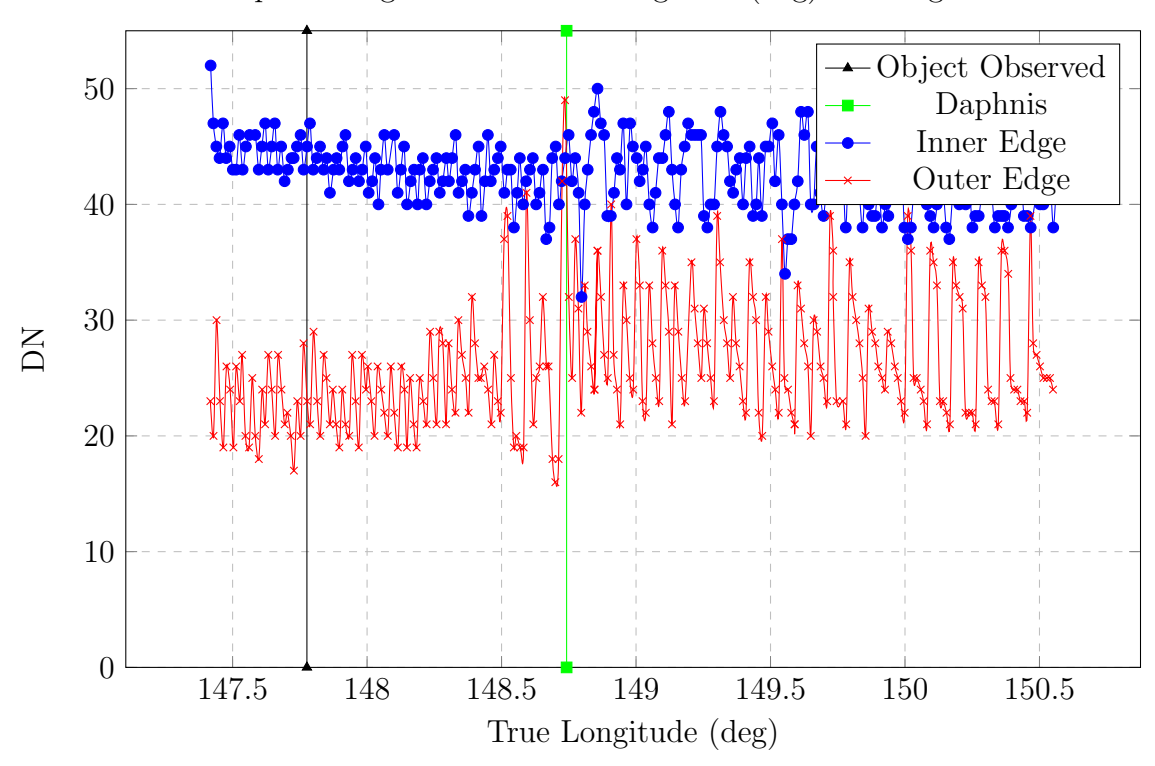


Figure 3.11.: N1591068064 Image Credit: NASA/JPL-Caltech/Space Science Institute

3.3.1. N1612090521: DN vs True Longitude graph

Fig. 3.3.1 is a plot of data collected from image N1612090521 which is labelled as Image H in section 3.1. Details for Image H can be found in Table 3.1. In Fig. 3.3.1, we see oscillations in the DN value at all points but there are clear increases in amplitude. The disturbance starts in the outer edge only. At true longitude greater than where Daphnis is located (148.741857), we see an increase in oscillations at the inner and the outer edge of the Keeler Gap. This was not expected as the oscillations should only be on the inner edge. A shadow from the waves on the opposing edge is only possible if Sun was in the same direction as Saturn is, from the perspective of the camera, almost eclipsed by Saturn. This doesn't appear to be the case. This could be due to an error in the method for acquiring data. The Keeler Gap is not entirely circular but in order to take measurements at regular intervals of true longitude, a ring was plotted using the rings tool in Caviar. This plots a specified of evenly distributed points at a specified radius. Since Daphnis' orbit and the Keeler Gap are eccentric, the ring points intended to be visible at the ring edge instead go into the disc of the A ring of the gap itself. The result is that the DN values along this line no longer show the oscillations of the Keeler gap edge but rather across the density wave at an angle. This can be corrected by eye. At each cross plotted by Caviar, move in the radial direction to maintain path along Keeler Gap edge. This ensures that measurements are still taken approximately uniformly but also stay along the Keeler Gap edge. This can usually be avoided by using an image that is of higher resolution so that the change of the radius of the Keeler Gap is less significant from one side of the image to the other. However we can see from the image that the oscillations are not as simple as a sinunsoidal wave.





3.3.2. N1630270620: DN vs True Longitude graph



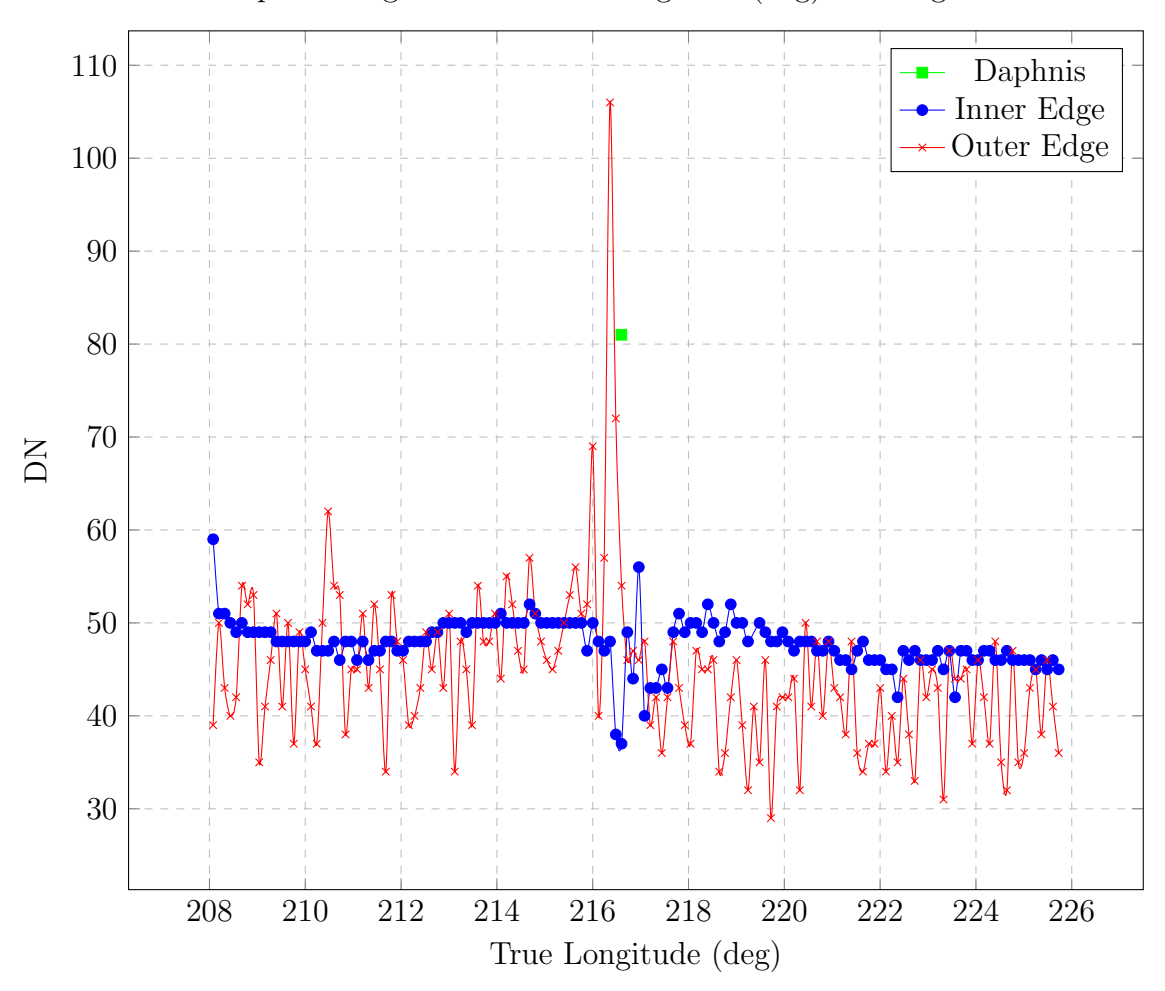


Image N1630270620 was taken on 2009-241 at 20:14:40. It was targeting rocks(Daphnis). The exposure was 680ms and has a radial resolution of 15.18913km/pixel. Fig. 3.12 is a plot of the inner edge of the Keeler Gap, showing how the Digital Number (DN) values change as a function of true longitude. There is an anomalous point at the 208°. This can be disregarded as this is due to reaching the edge of the image. We can clearly see an oscillation in the region of Daphnis that decays with respect to distance. What is interesting is that on the other side is a slight increase in oscillation. Looking at Fig. 3.13, we see the expected spike and decay at lower amplitudes. This is to be expected as this spike in amplitude occurs at Daphnis' location. There is another spike at the same true longitude as we saw in Fig. 3.12. This indicates that either the mechanism for damping of the Keeler Gap waves is not the same as previously thought or another object is present (even if not visible in the image). It is certainly interesting that the oscillation starts in the outer edge and then in the inner edge, as it does near Daphnis, but it does not have a corresponding spike like for Daphnis. However errors associated with DN values are approximately equal to

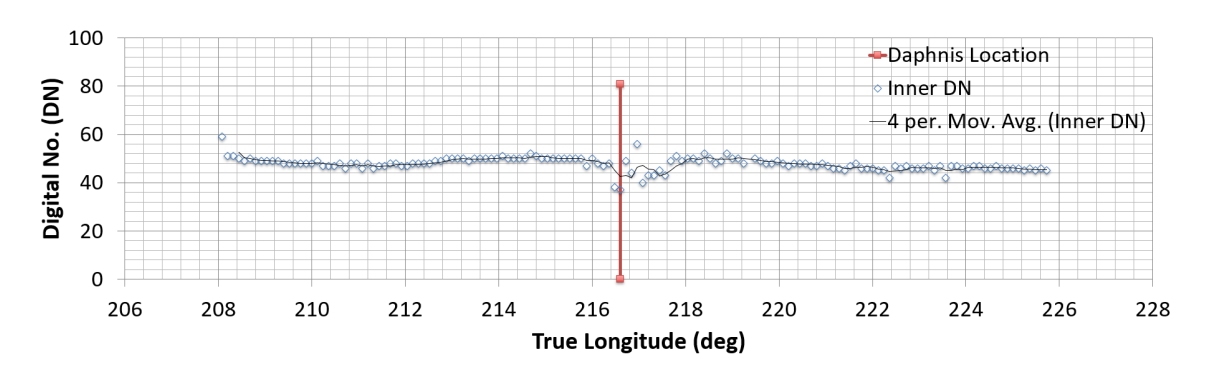


Figure 3.12.: Image N1630270620: Inner edge DN values

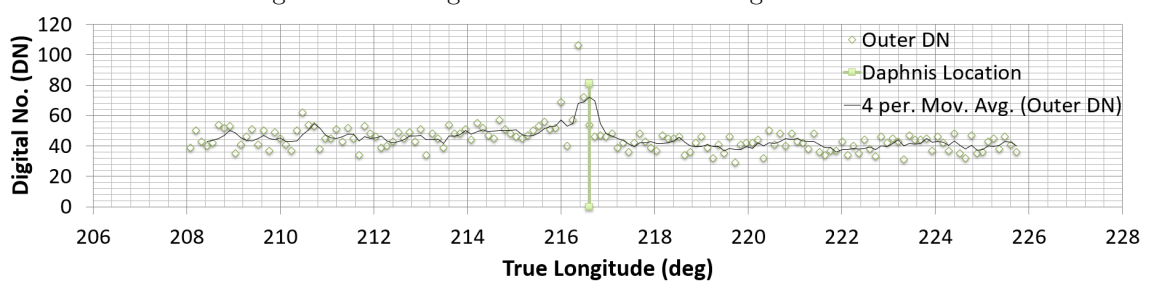


Figure 3.13.: Image N1630270620: Outer edge DN values

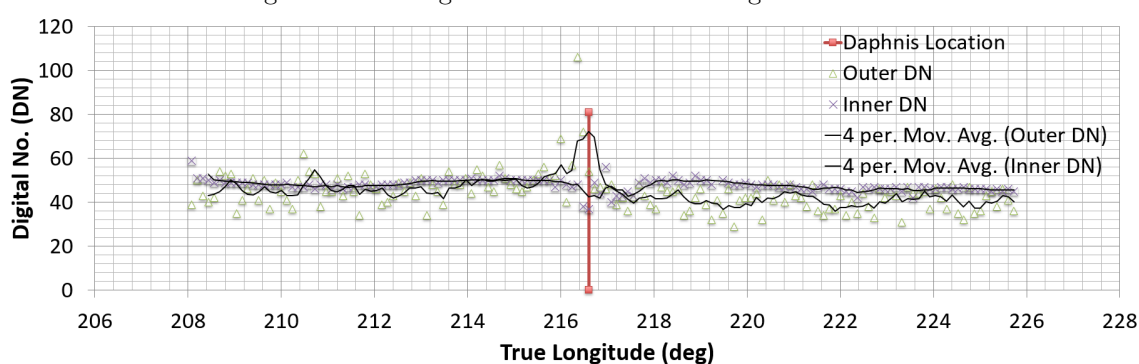


Figure 3.14.: Image N1630270620: Both inner and outer edge DN values

the size of disturbance, making conclusions difficult.

3.3.3. Motion of peak between subsequent images

To test whether this is a mechanism of damping or a new object, we look at a subsequent images to see whether this anomalous region moves relative to Daphnis. If it is Daphnis related, it must move at the same rate as Daphnis. If it is a new object it may move at a slightly different rate. Therefore we look to the next image to see if this disturbance can be found there as well and if it has moved relative to Daphnis. The next image is N1630270653.

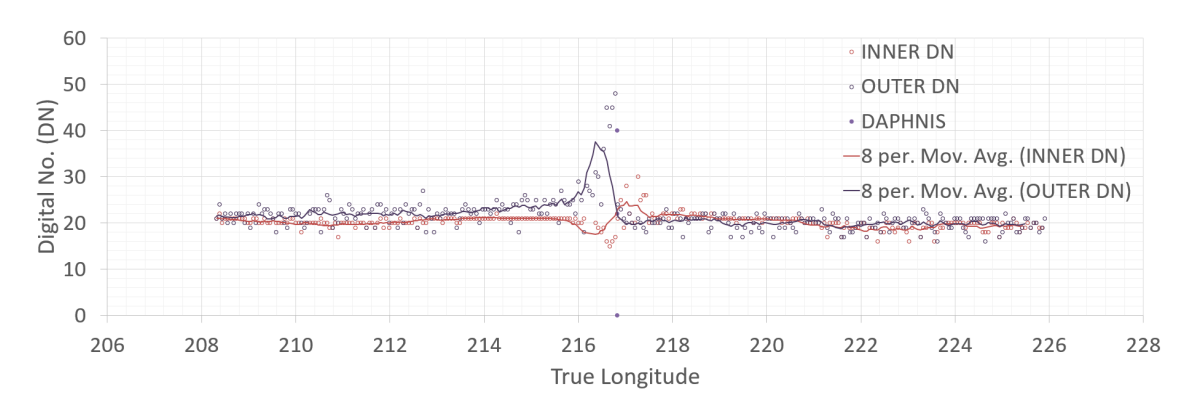


Figure 3.15.: A scatter plot of digital no. vs true longitude (deg) for image N1630270653. Both inner and outer edge DN values with moving averages

3.3.4. N1630270653: DN vs True Longitude graph

A scatter plot of digital no. vs true longitude (deg) for image N1630270653

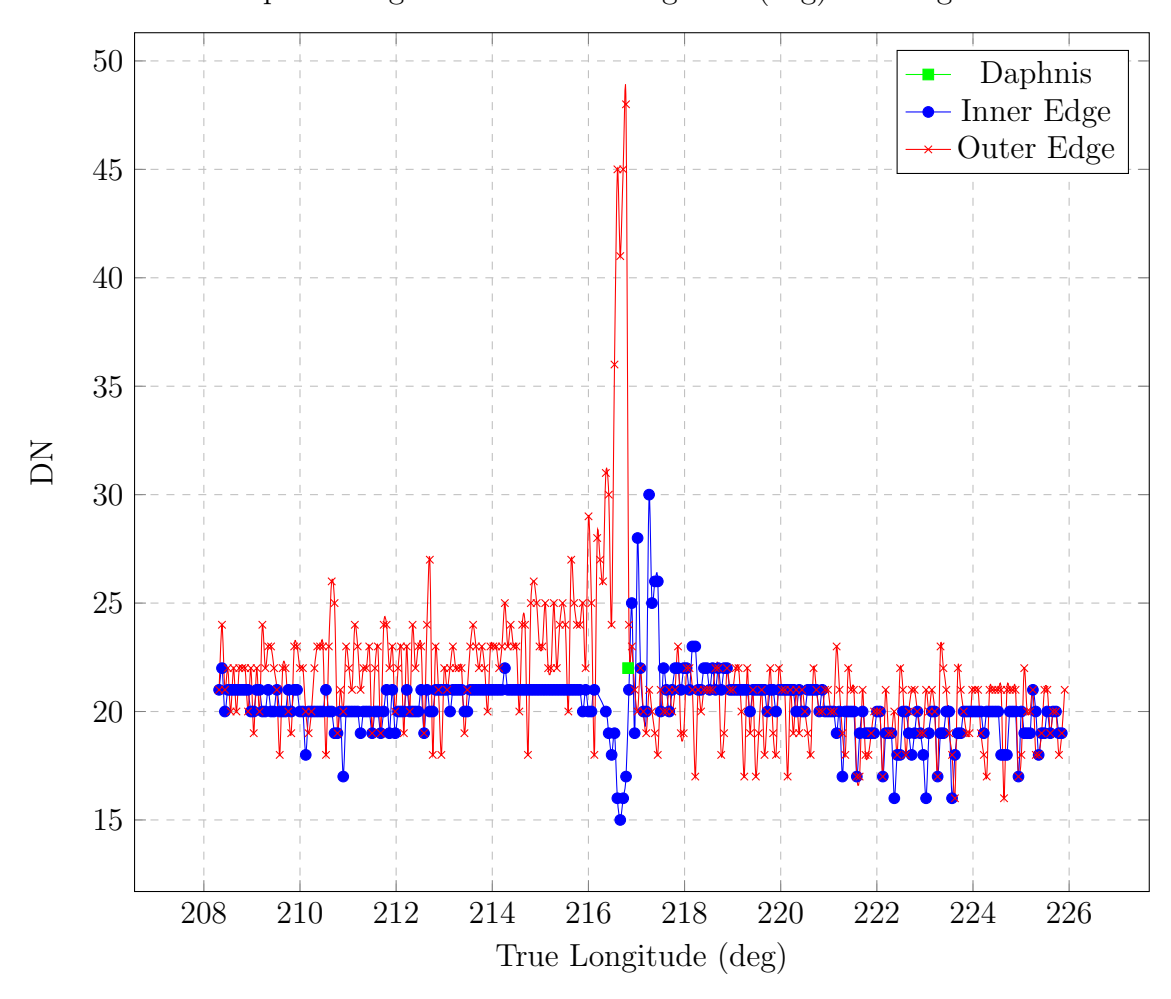


Image N1630270653 was taken on 2009-241 at 20:15:13. It was targeting rocks(Daphnis). The exposure was 150ms and has a radial resolution of 15.30661km/pixel. Fig. 3.15 and

Fig. 3.3.4 are graphs with the same data points but Fig. 3.15 is a scatter graph with the moving average as the trendline. At $\sim 210.7^{\circ}$ and $\sim 212.7^{\circ}$. A new one has appeared between the two original ones although there is no corresponding change by the new peak in the outer edge. If the first spike ($\sim 210.7^{\circ}$) is causing a shadow on the inner edge, creating a corresponding dip, then why isn't the new spike, despite being greater. One possibility is that inner edge variation is just due to random variation and neither of the spikes on the outer edge are causing a shadow on the inner edge. Another possibility is that the an object is causing a disturbance on the inner edge and that object is balancing the effect of the shadow. This would explain the lack of spike but it would also help to explain the actual anomalous point further down at $\sim 214^{\circ}$.

3.4. Mosaics

By creating mosaics, we can get a broader overview of the Keeler Gap. Mosaics are created by using a routine that reads a Batch List file and stitches the images together according to their relative position. A Batch List file is a text file that includes the Image Name, start true longitude and end true longitude of every image to be included in the mosaic. This requires use of the IDL programming language.

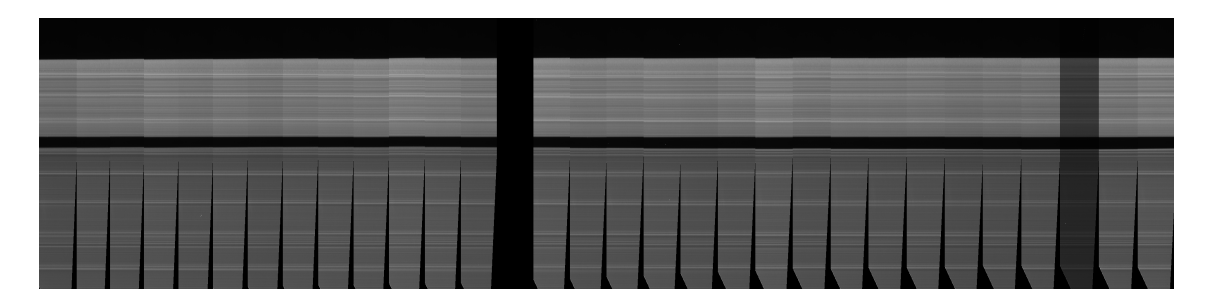


Figure 3.16.: Mosaic of Images N15849733717-N1584976298

N158497* Mosaic Fig. 3.16 is a mosaic of images showing True Longitude 91.6-98.4°with image. It has a radial range of 136,000 - 137,000km. Images included in this mosaic are all images taken between (inclusive) Image N15849733717 and Image N1584976298. The images were taken on 23rd March 2008. The start time was 13:50:09 and the end time was 14:36:08. The gap in the mosaic is due the image being unpointable. Another had a different exposure duration to the others and therefore appeared of be dimmer. This mosaic appears to show several bright regions in the mosaic of Keeler Gap. We know that none of these objects are Daphnis

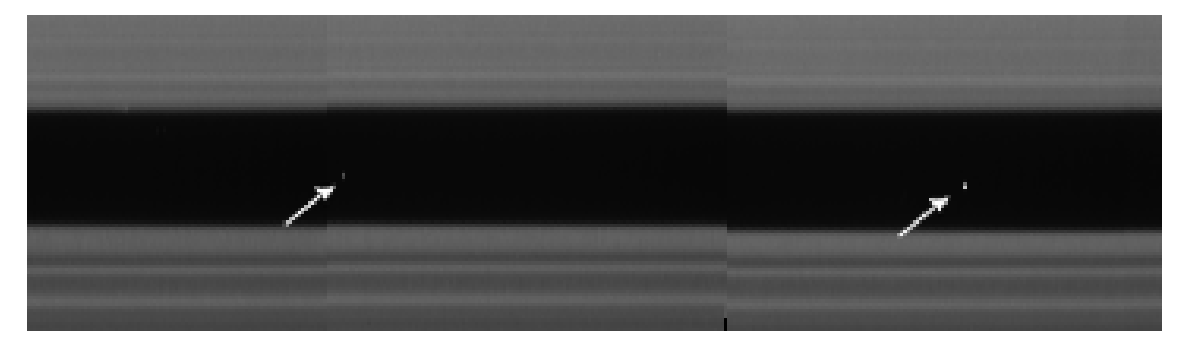


Figure 3.17.: Mosaic of Images N15849733717-N1584976298 (cropped)



Figure 3.18.: As a comparison, this is what a group of three stars looks like from another image (before reprojection) in the same sequence, Image N1584974696 Image Credit: NASA/JPL-Caltech/Space Science Institute

because 1. Daphnis' location prediction using the method described in section 2.4 2. These images have all been pointed and the Caviar Software does not predict Daphnis to be visible in these regions at the time the images were taken. These images were added to Table 3.1 as E and F and the mean motion was calculated between the two bright dot. It was concluded that these are not the same object as the true longitude could not changed that much in such a short amount of time. This is discussed further in subsection 3.5.5.

3.5. Discussion

3.5.1. Mass and Radius Constraints

The lower bound value for the radius of a potential new object was calculated to be 590 ± 360 m. This is large enough that it should be visible in high resolution images

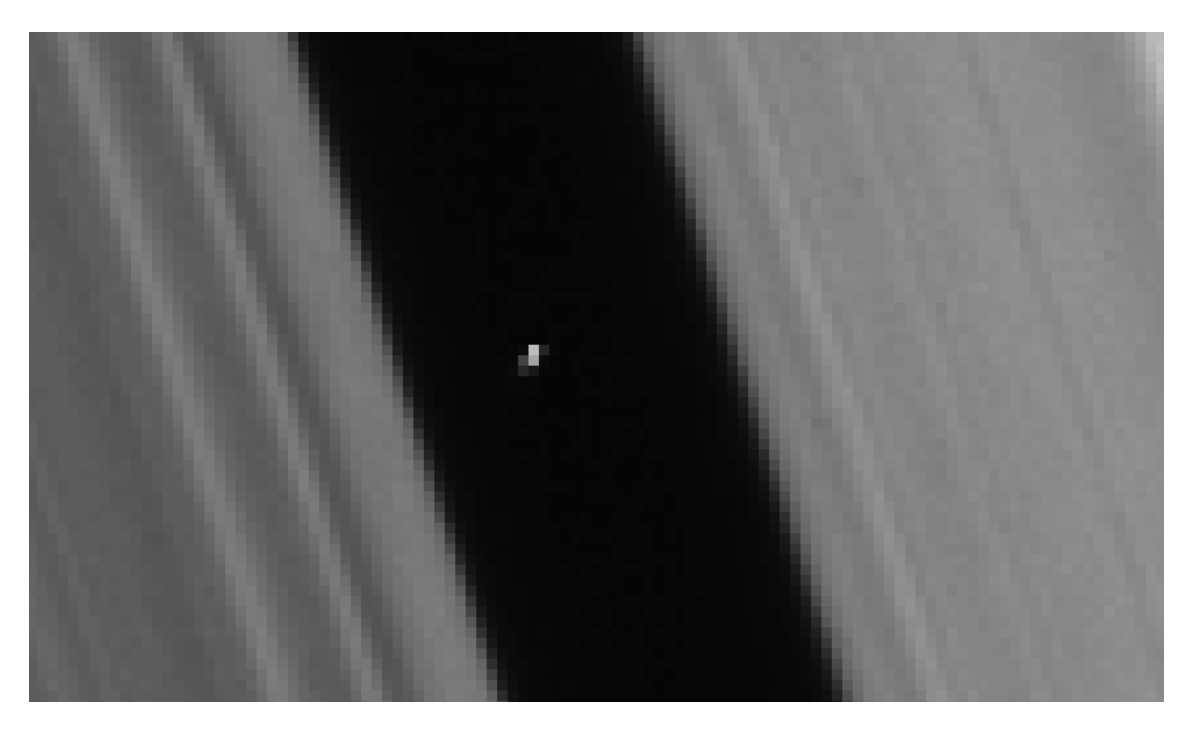


Figure 3.19.: Image N1584978784 (cropped)

(3700 km/deg). With the assumption that any other object in the gap should have similar density, we calculated an approximate value for the mass, $2.9 \pm 0.4 \times 10^{11}$ kg.

3.5.2. DN vs True Longitude Graphs

DN value depends on phase angle, albedo, location of the object (e.g. in the shadow of another feature). We are not looking at absolute values of DN. We are looking for relative, not absolute changes. The graphs produced suggest that damping is not as expected. While it initially decays, the amplitude increases again and this appears to match with a similar effect in the other direction on the opposite edge. This would suggest that it is getting an additional kick from another massive object. This echoes the findings of Weiss et al[5] that found that the analytic expression (relating the amplitude of the waves to the mass) over-estimated the mass of Daphnis by $\sim 30\%[5]$. No additional object can be seen in this image. This could be due the geometry of the image (e.g. the wave itself obscuring the gap partially). It could also be due to turbulence of the Keeler Gap edge particles. This could be explored further with the aid of a simulation. This would be a topic for future research.

3.5.3. Mosaic

When creating mosaics we specify the mean motion. Since Daphnis is in the Keeler Gap, and objects following Kepler's law in this region should be travelling at approximately the same speed. Therefore, Daphnis's mean motion is a reasonable estimate of the mean motion of another object in the Keeler Gap. All bar one of the images that make up this mosaic have an exposure duration of 680ms. The background stars appear to have been uniformly distorted due to the motion of Cassini during the exposure time. The geometry means that any objects that are in the target area (Keeler Gap) would appear stationary while (due to a parallax effect) anything further would appear to have drawn out a line in that time. Therefore any apparent circular objects would have to be near Saturn's disc. This could mean above and below. The two bright regions that appear in the gap as seen in Fig. 3.17 are likely to be located within Saturn's orbit. This is assuming that they are not due to random error. Upon closer inspection in Fig. 3.19 we see that there are approximately 5 brighter pixels, following a point spread function type pattern. Given the resolution of this image, this gives us an estimated radius of 1.48±0.74km. Assuming similar density, we would calculate the mass to be approximately $4.96 \pm 0.62 \times 10^{12}$ kg. For a mass this big intuitively we would expect to see waves in the Keeler Gap edge but it is not only the mass that affects the waves. It is the distance to the edge of the Gap which would be greater given the smaller radius[5]. Since Weiss et al noticed that the waves overestimated the mass of Daphnis by $\sim 30\%[5]$, it is not as simple as using an equation. In order to check what waves we should expect from a mass this big, we would create a simulation. This is a topic for future research.

3.5.4. Other images

Many images appear to have bright regions in the Keeler Gap. The majority of the images only have a couple of pixels that are brighter than the background. Only a few images and potential candidate that is 4 pixels or more. These images are shown in Fig. 3.5a, Fig. 3.19, Fig. 3.11 and Fig. 3.3b. For the rest of the images, it is very difficult to distinguish from cosmic rays that can appears as anything from bright pixels to "squiggle-shaped" lines. This is why it is important to be able to track the object and to exclude anomalies.

3.5.5. Mean Motion

The calculations were tested with Daphnis observations giving a good indication of the errors that may be associated with the tracking method. The error in the calculated mean motion increases with time as expected, making them less reliable. It is also worth noting that if two random bright pixels (e.g. a cosmic ray) appear in an images that are both targeted at Daphnis, then inevitably, it would appear to have a similar mean motion by then mere fact that it the range of true longitudes observed is limited. The mean motion's of I-J, G-H, H-I and C-D seem to the be only ones that don't suffer from the errors associated, catastrophically. The others have errors that are too great to consider at this stage although as the candidate list expands, these images could contribute to future calculations. After comparing the mean motions, we look to compare the images themselves of the candidates.

- **E-F** Images labelled I and J (shown in Fig. 3.3b and Fig. 3.11 respectively) have a mean motion of $-403.7897384 \pm 0.415031971$ Image I and J do not show the same object, given the mean motion. What it does suggest is that there are two objects in near proximity, neither of which are Daphnis nor catalogued background stars. Given the quantity of pixels, it is also unlikely that these are cosmic rays.
- I-J Images labelled I and J (shown in Fig. 3.7 and Fig. 3.8 respectively) have a mean motion of $597.151419 \pm 2.595559907$ The mean motion and the error are much more plausible for an object in the Keeler Gap although slow. The mean motion is comparable to Altas which has a mean motion of 598.312351[2].
- G-H Images labelled G and H (shown in Fig. 3.5a and Fig. 3.6b respectively) have a mean motion of $605.006719 \pm 16.68948037$ deg/day. Although the images were taken one Daphnis orbit apart with a mean motion very similar to that of Daphnis. The phase angle is approximately same so it should look similar. The DN value measured for G is double what is measured for H. This could be related to motion perpendicular to the plane of the disc, a varying inclination. The phase angle for Image G is 42.673 and the phase angle for Image H is 58.5. This is a significant change and would explain a difference in appearance. They could also be different objects or anomalies as these are both Daphnis targeted images.
- **H-I** Images labelled H and I (shown in Fig. 3.6b and Fig. 3.7 respectively) have a mean motion of $569.8484177 \pm 218.6303506 \text{ deg/day}$. They appear to have a similar

size and appearance. Although the error is large and the mean motion calculated is too low for it to be in the Keeler Gap (comparable to Pandora at 572.788589[2]), it is still possible that these are the same object in the Keeler Gap (albeit less likely).

G-I Images labelled H and I (shown in Fig. 3.5a and Fig. 3.7 respectively) have a mean motion of $571.9682596 \pm 244.6032208$ deg/day. Image G and I look similar in the image and have a similar radii.

C-D Images labelled C and D (shown in Fig. 3.19and Fig. 3.2 respectively)have a mean motion of $605.5184465 \pm 205.3882713$ deg/day. There is a very significant error for this mean motion however it a value that is very similar to what we would expect for an object in the Keeler Gap. Fig. 3.2 has a longer exposure (1000ms instead of 680ms). This makes visual comparisons more challenging. The difference in appearance would suggest that these are not the same object.

4. Conclusion

To conclude, we analysed many different aspects of the Keeler Gap using Cassini images. First, we conducted a strategic search to find images of the Keeler Gap with and without Daphnis present. We then selected images amongst these that appeared to show interesting features. They appeared to be in the Keeler Gap so assuming that they are travelling with a similar mean motion to Daphnis, we calculated the new locations of these bright regions at the time that new images were taken. This was much more difficult that anticipated as Cassini camera images have been taken and the camera is almost always facing a different direction at the time that the image was taken, to what we require to observe the object. Since we had multiple examples of bright regions we were able to calculate mean motions between them. This makes the assumption that they are all the same object. Most of the pairs yielded mean motions that were comparable to Daphnis. This was mostly due to the fact that when images were taken a long time apart, the number of orbits in between was not known. To complete the calculation an assumption was made that the number of orbits that an object in the Gap would have made in that time, should be equivalent to the number of orbits made by Daphnis. The greater the number of orbits, the greater weighting on Daphnis' mean motion and therefore tends towards an equivalent value. Another pair (E-F) had a starkly different mean motion compared to the others, despite the images being taken minutes apart. This could either be due to cosmic rays, certainly these are not the same object. Image pairs I-J, G-H, H-I, G-I and C-D gave promising results. They all appear near Daphnis at approximately the time that Daphnis' orbit is thought to have changed[3]. This leads to the possibility that G, H and I are all the same object but definitive conclusions are difficult to draw given the significance of the error. This would require further investigation.

Having noticed an anomalous increase of amplitude of Daphnis' decaying outer edge wave, we plotted a graph of DN vs True Longitude to see if this anomaly was also apparent on the inner edge of the Keeler Gap. The graphs showed a minor disturbance in the same area on the inner edge. Given that DN values are integers and

the DN changes by 1 or 2, this could be a coincidence.

To scan large areas of the Keeler Gap, we created re-projections of the Keeler Gap images and stitched them together forming a mosaic. This appeared to show bright dots in the Keeler Gap. These were added to the list of candidates and images E and F.

During the initial search, we were able to track a dot across consecutive images. At first, it seemed that this was an object in the Keeler Gap but mean motion calculations led us to believe that this was highly unlikely to be the case. The mean motion was far too low. It is unlikely to be a background star given the small variations in the RA and Dec. It is unlikely to be a cosmic ray given its appearance and consistency across consecutive images. A possibility is that is another object within the solar system or in distant orbit and inclined orbit around Saturn.

In addition, we know that two bright regions that were observed from the mosaic we produced appear to to be within the Keeler Gap and are not the same object as the mean motion, n, would be \sim -403 \pm 0.32°/day. There is a lot of evidence that has indicated that there is an object as yet undiscovered in the gap[5][3]. Further research is required to find it or find them all if there are multiple objects present in the Keeler Gap.

4.0.1. Future Research

It is not just the predictions of whether any objects in view that are of importance but also what is not and the likelihood of false positives. A statistical analysis of cosmic rays and other features would be a useful area of future research to simply allow us to determine the significance of anomalous pixels. The mosaic and the individual images suggest multiple candidates instead of one. To test this, we would need to calculate all mean motions between pairs of images. Since there are so many images to search through, it is likely that many relevant images have been missed. We found in one case that there was an untargeted image of Daphnis, perfectly in view as if it had been the target, searching for more would certainly be helpful to better understanding Daphnis' behaviour. If not finding new candidates, this would help rule out any interaction with Daphnis.

We could look further into the unusual decay of the edge waves and assess whether it is systematic error (due to using a circular guide on an elliptical ring edge), turbulence of wave particles or random error. We would do this by reprojecting the image to ensure that each row corresponds to a constant radius. Then use a matrix of all DN values and plot a 3 dimensional graph and see whether there is a radial component to this spike as there would be if there was an actual wave present instead of random error. By using a matrix, we can exaggerate peaks and trough and check particular cross sections much faster. Creating a simulation of edge waves to test decay and possible turbulence, would help determine whether this spike could be caused by Daphnis alone.

Jacobson calculated that the mean motion changed twice[3], giving us 3 values for the mean motion. This may be connected to the 4 ridge lines that can be seen on Daphnis. A hypothesis to test is whether the ridge lines are equatorial ridges and are they related to each other in a predictable way, i.e. linked to the orbit. To establish whether this is the case, further images from different angles and a simulation may be useful. To summarise, the case is not closed, there are many avenues to explore to help tie together all these features.

Bibliography

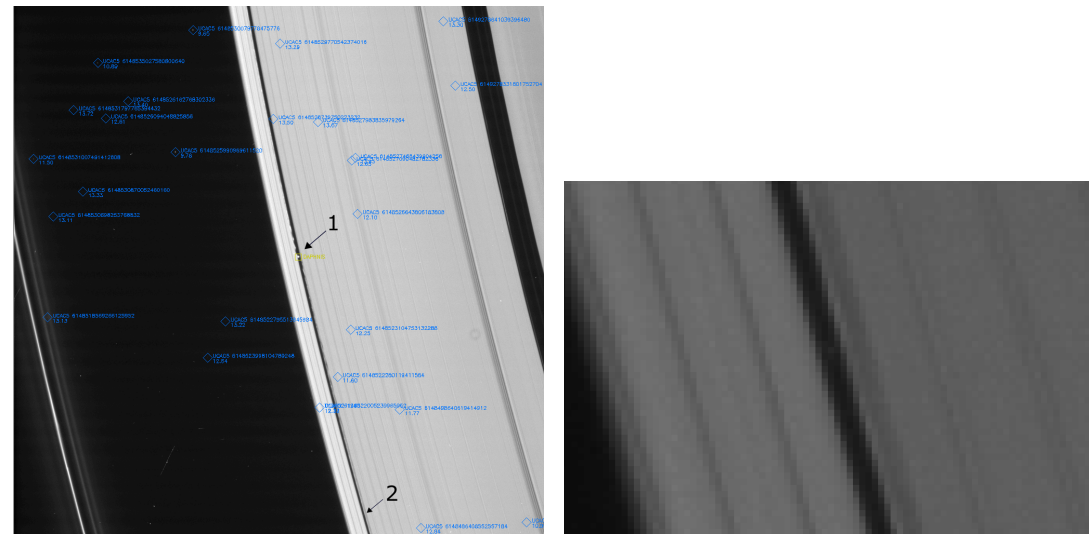
- [1] Cassini imaging science: Instrument characteristics and anticipated scientific investigations at Saturn.
- [2] Jacobson R. A. Revised orbits of Saturn's small inner satellites. *Astronomical Journal*, 135, 2008.
- [3] Jacobson R. A. Daphnis sat393, 2016. JPL/Caltech, internal memo, 2016.
- [4] Thomas P. C. Sizes, shapes, and derived properties of the saturnian satellites after the Cassini nominal mission. *Icarus*, 208, 2010.
- [5] Weiss J.W., Porco C.C. and Tiscerano M.S. Ring edge waves and the masses of nearby satellites. *Astronomical Journal*, 138:272–286, 2009.
- [6] Charnoz S. et al. The Equatorial Ridges of Pan and Atlas: Terminal Accretionary Ornaments? *Science*, 318, 2007.
- [7] Cooper N.J. et al. The Caviar software package for the astrometric reduction of cassini iss images: description and examples. $A \mathcal{E} A$, 610, 2018.
- [8] Hedman M. M. et al. Of horseshoes and heliotropes: Dynamics of dust in the encke gap. *Icarus*, 212, 2011.
- [9] Porco C.C. et al. Saturn's small inner satellites: Clues to their origins. *Science*, 318, 2007.
- [10] Tajeddine R. et al. Dynamical phenomena at the inner edge of the keeler gap. *Icarus*, 289, 2017.
- [11] Dermott S. F. Dynamics of narrow rings. *Planetary rings*, 1984.
- [12] California Institute of Technology Jet Propulsion Laboratory. Cassini legacy, 2018. https://saturn.jpl.nasa.gov/.
- [13] California Institute of Technology Jet Propulsion Laboratory. Voyager, 2018. https://voyager.jpl.nasa.gov/.
- [14] Cooke M.L. Saturn's rings: Photometric studies of the C Ring and radial variation of the Keeler Gap. PhD thesis, Cornell University, Ithaca, NY, 1991.
- [15] Murray C.D., Dermott S. Solar System Dynamics. Cambridge University Press, 2000.

- [16] NASA. Opus data search for outer planets NASA mission data NASA PDS ring-moon systems node, 2018. https://tools.pds-rings.seti.org/opus/.
- [17] Planetary Science Communications team at NASA's Jet Propulsion Laboratory and Goddard Space Flight Center. NASA science; solar system exploration, 2017. https://solarsystem.nasa.gov/moons/saturn-moons/.

Appendices

A. Other Images

These are the images of candidates that were not directly discussed in the report but were included so that visual comparisons can be made to the other candidates.



- (a) Image K with each star and Daphnis la-(b) Image K (cropped and magnified) with pobelled using Caviar. Arrow 1 = Daphnis, Arrow 2 = potential candidate. Image Credit: NASA/JPL-Caltech/Space Science Institute
 - tential candidate at the centre of the image within the gap. Image Credit: NASA/JPL-Caltech/Space Science Institute

Figure A.1.: For image details, see Table 3.1.

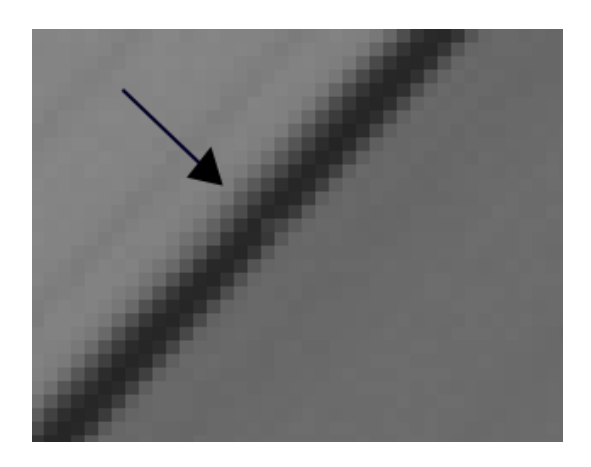
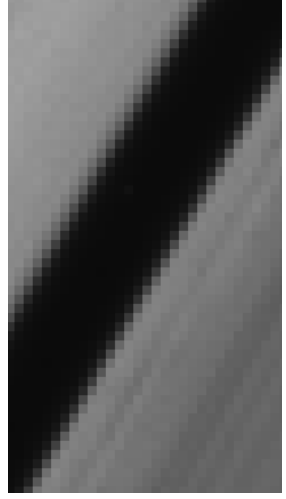
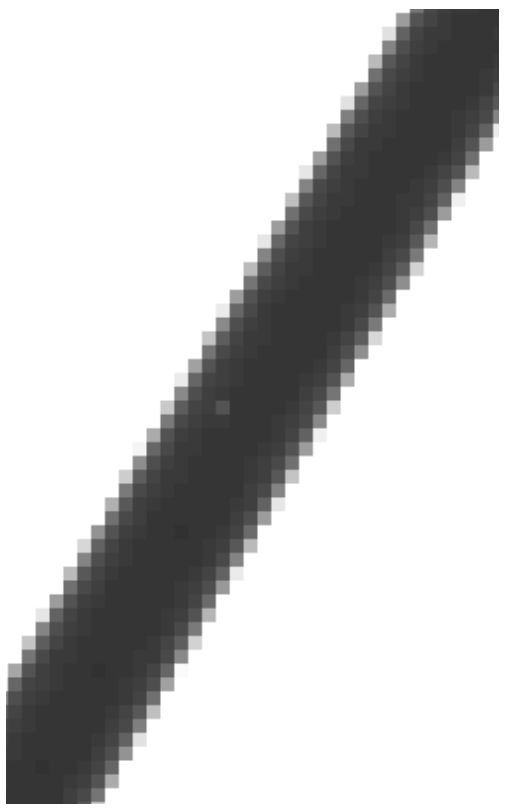


Figure A.2.: Image L. In this image the variation is barely visible due to the low resolution of the image. For image details, see Table 3.1. Image Credit: NASA/JPL-Caltech/Space Science Institute



(a) Image M (cropped)
Image Credit:
NASA/JPLCaltech/Space
Science Institute



(b) Image M (cropped and stretched) crop of N1743631128 Image Credit: NASA/JPL-Caltech/Space Science Institute

Figure A.3.: This image had to be stretched (as seen in Fig. A.3b) significantly in order to see the single anomalous pixel. This is very unusual. However the DN value measured for this pixel is second highest of the candidate images. The DN value of the pixel is 218. For image details, see Table 3.1



Figure A.4.: Image A (cropped), For image details, see Table 3.1. Contribution from Dr N. J. Cooper (personal communication). Image Credit: NASA/JPL-Caltech/Space Science Institute

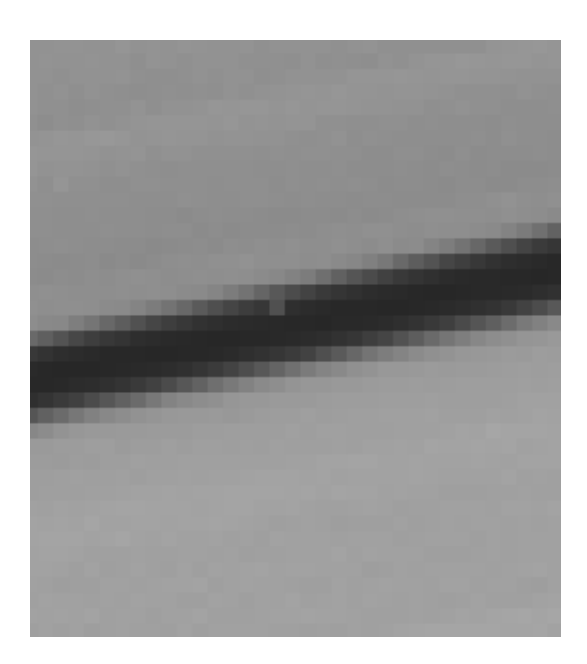


Figure A.5.: Image B (cropped), For image details, see Table 3.1. Image Credit: NASA/JPL-Caltech/Space Science Institute

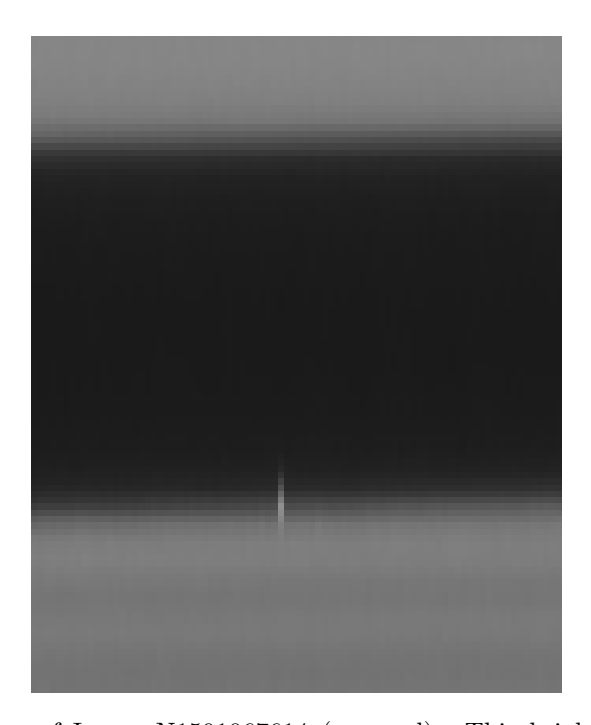


Figure A.6.: Reprojection of Image N1591067614 (cropped). This bright line is approximately circular in appearance in the raw image but the reprojection process of the image has distorted it.